Spondias mombin flavonoids showed super-binder ability with Downstream Molecular Targets of Parkinson's Disease: Folkloric-therapy assessment as a Scaffold for Structural Studies in Neurodegenerative disease

John A. Olanrewaju

Department of Biocomputing, Eureka Research Laboratory, Department of Anatomy, Faculty of Basic Medical Science, Benjamin Carson (Snr.) School of Medical Science BABCOCK University Ilishan-Remo, Ogun State, Nigeria. https://orcid.org/0000-0002-9540-4117

Leviticus O. Arietarhire

Department of Biocomputing, Eureka Research Laboratory, Department of Anatomy, Faculty of Basic Medical Science, Benjamin Carson (Snr.) School of Medical Science BABCOCK University Ilishan-Remo, Ogun State, Nigeria. https://orcid.org/0000-0003-4069-0950

Oladimeji E. Soremekun

Department of Biocomputing, Eureka Research Laboratory, Department of Anatomy, Faculty of Basic Medical Science, Benjamin Carson (Snr.) School of Medical Science BABCOCK University Ilishan-Remo, Ogun State, Nigeria. https://orcid.org/0000-0001-6086-7616

Ezekiel A. Olugbogi (**olugbogiezekiel@gmail.com**)

Department of Biocomputing, Eureka Research Laboratory, Department of Anatomy, Faculty of Basic Medical Science, Benjamin Carson (Snr.) School of Medical Science BABCOCK University Ilishan-Remo, Ogun State, Nigeria. https://orcid.org/0000-0003-1415-8856

Toluwanimi O. Afolabi

Department of Biocomputing, Eureka Research Laboratory, Department of Anatomy, Faculty of Basic Medical Science, Benjamin Carson (Snr.) School of Medical Science BABCOCK University Ilishan-Remo, Ogun State, Nigeria. https://orcid.org/0000-0003-3603-3392

Babatunji E. Oyinloye

Institute of Drug Research and Development, SE Bogoro Center, Afe Babalola University, PMB 5454, Ado, Ekiti, 360001, Nigeria. https://orcid.org/0000-0003-2165-7936

Olaposi I. Omotuyi

Institute of Drug Research and Development, SE Bogoro Center, Afe Babalola University, PMB 5454, Ado, Ekiti, 360001, Nigeria. https://orcid.org/0000-0002-5473-745X

Steven Russell

Department of Genetics, University of Cambridge, United Kingdom. https://orcid.org/0000-0003-0546-3031

Research Article

Keywords: Parkinson's Disease, Neurodegeneration, CADD, Spondias mombin, folkloric therapy, and drug optimization

Posted Date: December 29th, 2023

DOI: https://doi.org/10.21203/rs.3.rs-3815017/v1

Additional Declarations: The authors declare no competing interests.

Abstract

Spondias mombin (*S. mombin*), a prominent botanical resource, has garnered recognition within folkloric therapy. Parkinson's disease (PD), characterized by dopaminergic neuron attrition in the substantia nigra, manifests as motor anomalies like tremors, rigidity, and bradykinesia. This study capitalizes on *S. mombin*'s reservoir of 100 characterized phytocompounds and employs computational methodologies to interrogate their potential 35 PD-associated target proteins. Employing a multifaceted approach, we engaged in molecular docking, ADMET predictions, Molecular Mechanics/Generalized Born Surface Area (MM/GBSA) evaluations, Density Functional Theory (DFT), and Molecular Dynamic Simulations (MDS). This comprehensive framework facilitated insightful structural assessments and predictive analyses. Impressively, flavonoids hailing from *S. mombin*, including quercetin, catechin, ellagic acid, and epicatechin, showcased optimal binding affinities for PD-relevant target proteins. Moreover, these identified ligands exhibited minimal signs of mutagenicity, tumorigenicity, or irritancy, except for quercetin, which displayed elevated tumorigenic potential. Notably, quercetin and dopamine exhibited varying band gap energies, with quercetin the lowest (3.63 eV) and dopamine the highest (5.76 eV) values. MDS result suggests a synergistic outcome based on the RMSD and RMSF graphs for quercetin highlighting it as the best of all including the co-ligand. In a collective sense, our findings present *S. mombin* as promising reservoirs of active pharmaceutical ingredients, warranting further exploration for novel PD therapeutic avenues. Consequently, this study underscores the enhanced efficacy of phyto-ligands sourced from *S. mombin*, advocating their optimization as potential drug candidates.

Introduction

Lewy bodies accumulate within the midbrain in Parkinson's disease (PD), a neurological disorder characterized by the degeneration of dopaminergic neurons, primarily in the substantia nigra. This degeneration leads to muscle tremors, rigidity, impaired balance, and bradykinesia (Poewe et al., 2017). PD has witnessed an alarming surge in prevalence, disability-adjusted life years (DALYs), and mortality rates, consequently imposing substantial economic and societal burdens globally (WHO, 2019). Over the past quarter-century, PD prevalence has doubled, with approximately 8.5 million cases reported worldwide in 2019 (WHO, 2022). Notably, PD exhibits an unprecedented escalation in disability and fatality rates compared to other neurological disorders (WHO, 2022). A study from 2019 revealed a surge of 81% in DALYs and 100% in deaths since 2000, amounting to 5.8 million DALYs and 329,000 deaths attributable to PD (WHO, 2022), and this trend is projected to persist in the near future.

Amid this landscape, research endeavors have intensively focused on deciphering the pathobiology of PD, highlighting mitochondrial dysfunction, inflammation, protein quality control failure, and autophagy impairment as underlying mechanisms (Whitworth et al., 2008). Moreover, genome-wide association studies (GWAS) have identified genetic factors such as SNCA, LRRK2, VPS35, PRKN, PINK1, DJ-1, and GBA as contributors to familial PD in developed nations (Bandres-Ciga et al., 2020). Nevertheless, the bulk of these investigations predominantly stem from Eurocentric and, to a lesser extent, Asiacentric perspectives, resulting in substantial knowledge gaps regarding PD's incidence, prevalence, genetic

underpinnings, clinical manifestations, and other critical aspects within regions like Sub-Saharan Africa (SSA) (Williams et al., 2018). This dearth of data hampers the pursuit of effective treatments and the reduction of the global PD burden.

To foster the development of PD therapeutic agents tailored to SSA, an innovative avenue for therapeutic discovery lies in the realm of African folkloric medicinal plants. Notably, the past decade has witnessed a burgeoning acceptance of medicinal herbs as complementary healthcare modalities (Ekor, 2014), with noteworthy clinical successes like Niprisan for sickle cell disorders and Virucidine for COVID-19 management, both products of the National Institute for Pharmaceutical Research and Development (NIPRID) (Obodozie et al., 2010; Omotuyi et al., 2021).

In contrast to Europe and Asia, where studies have explored herbal remedies such as *Atropa belladonna*, *Hyoscyamus niger*, *Lepidium meyenii*, *Asparagus racemosus*, *Mucuna pruriens L.*, and *Ginkgo biloba* for PD-like symptoms, African herbal treatments, particularly those from Crossyne Flava bulbs, *Boophone Haemanthoides*, and *Nerine humilis* (Amaryllidaceae), remain less explored despite their reported potential (Omotuyi et al., 2021). The present study capitalizes on the prior ethnobotanical survey of West African plants with implications for neurodegenerative diseases (Asiimwe et al., 2015). Through the application of the Use Mention Index (UMI), *Spondias mombin L.* has been identified as promising sources of active pharmaceutical ingredients (APIs) with potential efficacy in PD treatment. *S. mombin*'s compounds will be used to target some PD's target protein in this work (*Werner et al., 2021*).

Computer Aided Drug Design (CADD) emerges as a pivotal methodology in the pursuit of drug discovery for PD (Butcher et al., 2004; Baig et al., 2018). Leveraging computational techniques, such as Molecular docking, Molecular Dynamic Simulations (MDS), and Pharmacokinetic predictions, CADD offers a comprehensive platform to investigate the interactions between potential drug candidates and PD-associated target proteins (Salman et al., 2021). These target proteins, intricately involved in pathways relevant to neuroinflammation, oxidative stress, and protein aggregation, represent attractive points for therapeutic intervention.

Materials and Methods

Identification and Retrieval of Proteins

Studies have shown that the following proteins play important roles in the pathophysiology of PD (Table 1). All the mentioned proteins were retrieved in their 3D crystal structures from PDB in PDB file format and subjected to the protein pre-process module of Schrödinger Maestro 12.8 version. Their respective protein data bank (PDB) IDs are given in Table 1 in supplementary file 1 (SF1).

Preparation of Proteins

All 35 proteins implicated in this study were prepared using a protein preparation wizard which involved the assignment of bond orders and hydrogen bonds, addition of hydrogens, optimization, minimization of

the proteins, and deletion of waters beyond 4Å from the het group (Sastry et al., 2013). The SiteMap tool was employed for the determination of highly potential binding sites of ligands on proteins (Halgren, 2009). The proteins' receptor grids, which map the binding sites of these proteins for ligand binding, were generated by Glide application on maestro 12.8(Schrödinger, 2023).

Retrieval and Preparation of Phytocompounds

100 phytocompounds of S.Mombin were sourced after thorough literature search. These sourced compounds were retrieved from PubChem database (https://pubchem.ncbi.nlm.nih.gov) with the varying PubChem CIDs in structure data file format (MOL.SDF). They were prepared using LigPrep in the Schrödinger suite, where OPLS4 force field module was employed for minimization, they were desalted and retaining specified chiralities and adopting Epik to generate states of the chemical compounds at pH 7.0 ± 2.0 was carried out.

Molecular Docking Using Glide

Subsequent to receptors and ligands preparation, we conducted molecular docking computations utilizing Glide's ligand docking module. The process began with Standard-Precision docking (SP-docking), which is a less stringent method. This initial phase was crucial for filtering out ligands with high affinity prospects. Subsequently, the compounds that successfully passed this preliminary screening were advanced to the Extra-Precision docking (XP-docking) stage. This phase involved a more stringent assessment of the ligands' binding affinity, ensuring a thorough and precise screening process. Following the docking stages, we focused on evaluating the binding stability of the protein-ligand complexes. This was achieved through the calculation of the relative binding-free energy (ΔG bind) of the compounds exhibiting the best binding poses, identified as hit ligands by employing MM/GBSA using the Prime Module in Maestro (Borkotoky et al., 2016).

Pharmacokinetics Screening

The drug-likeness, physicochemical properties and pharmacokinetic properties of the hit chemical compounds from S. mombin were predicted by Qikprop, a plugin in maestro schrodinger, while they were screened for toxicity using Datawarrior program version 4.6.1 (Sander et al., 2015).

Density Functional Theory

The molecular characteristics of the hit compounds were evaluated via quantum chemical calculation using DFT to anticipate the biological activities of the top-ranked compounds. After the molecules underwent a conformer distribution calculation, the most stable conformer was picked for the DFT analysis in vacuum using Spartan 10 computational chemistry software. The thermodynamic parameters, EHOMO and ELUMO were computed. The global reactivity descriptors and other characteristics were generated from the EHOMO and ELUMO values. The energy band gaps were calculated from the difference between ELUMO and EHOMO (Eg).

Eg = ELUMO-EHOMO (1)

Koopman's theory connects the Ionization energy (I) and Electron Affinity (A) to EHOMO and ELUMO (Koopmans, 1993).

I = -EHOMO (2)

A = -ELUMO (3)

$\chi = 1+A / 2$ (4)

$\eta = 1-A / 2$ (5)

$\delta = 1 / n$ (6)

Molecular Dynamic Simulation

Molecular dynamics simulations (MDS) were performed using Schrödinger's Desmond module within the Maestro interface (Bowers et al., 2006; Schrödinger, 2023). The System Builder tool was employed to construct the simulation environment for the protein-ligand complexes, ensuring the correct protonation states and solvation. The systems were equilibrated and simulated for 200 nanoseconds (ns) in an isothermal-isobaric (NPT) ensemble class, stabilizing temperature, and pressure. Long-range electrostatic interactions were calculated using the Particle-Mesh Ewald method with a grid spacing of 0.8 Å, while Coulomb interactions were truncated beyond a 9.0 Å cut-off radius. The simulations aimed to elucidate the dynamic behavior and stability of the complexes, providing insights into the conformational changes and interactions over time. Data from MDS were analyzed for various parameters including root-mean-square deviation (RMSD), root-mean-square fluctuation (RMSF), and interaction profiling to assess the binding efficacy and structural integrity of the complexes (Olugbogi et al., 2023).

Result and Discussion

This study aims to elucidate the potential inhibitory and modulatory effects of bioactive compounds present in *Spondias mombin* against various targets implicated in Parkinson's disease (PD). Employing a multifaceted computational approach encompassing molecular docking, pharmacokinetic prediction, binding free energy analysis, and HOMO/LUMO assessment (Ajiboye et al., 2023), we sought to identify and characterize the interactions between these compounds and their respective protein targets. Through rigorous computational analyses, we successfully identified four bioactive phytocompounds derived from *S. mombin* that exhibit promising potential as lead ligands. These ligands demonstrated notable therapeutic implications through their interactions with eight protein targets associated with PD.

Our investigation revealed substantial molecular interactions and remarkable stability of the ligand-protein complexes formed. Intriguingly, a comparative evaluation between these bioactive compounds and the established co-crystallized-ligands for these proteins was conducted, yielding significant insights

that underscore the significance of our research endeavor. This study not only sheds light on the therapeutic prospects of *S. mombin*-derived compounds in tackling PD but also underscores the valuable contributions of computational methodologies in elucidating intricate ligand-protein interactions. As such, our findings contribute to the expanding field of computational drug discovery and hold promise for the development of novel interventions for PD.

Molecular docking Study

Following the execution of molecular docking simulations encompassing 100 phytocompounds extracted from *S. mombin* against a comprehensive set of 35 proteins associated with Parkinson's disease (PD), a subset of four compounds emerged exhibiting notably improved docking scores compared to the co-crystallized ligands found within the proteins. Within this subset, eight proteins exhibited robust intermolecular interactions with these identified hits, while the remaining proteins either exhibited low affinities or no affinities at all with the *S. mombin* phytocompounds. The outcome of this investigation is presented in Table 2, and the spatial distribution of binding affinities is visualized through heat maps (Figure 1) and graphical representations (Figure 2a).

Notably, the results in Table 2 and Figure 1 underscore the particularly high binding affinities observed when the hit ligands interacted with the phosphoinositide-3-kinase protein. Specifically, ellagic acid achieved the highest binding affinity score of -10.466 kcal/mol, suggesting the potency of this protein as a prospective novel target in PD therapy. Additionally, JNK2 emerged as another significant target, demonstrating substantial binding scores and robust interactions with the hit compounds, closely followed by Pi3k and A2 receptor, as detailed in Table 1 and Figure1 and 2a-b.

The study's findings emphasize the consistent and elevated interactive capacities of quercetin and ellagic acid, evident from their binding scores not falling below -7.0 kcal/mol when docked with six and eight of the lead targets, respectively (Table 1). This resilience suggests their potential to disrupt the pathways associated with these lead targets, positioning them as promising small-molecule candidates for the long-term management of PD.

Further exploration of ligand-protein complex stability during the docking simulations strengthens the study's conclusions. Table 2 and Figure 2b present the free binding energy scores, measured in kcal/mol, for the identified hit ligands. Notably, ellagic acid consistently exhibited high complex stability across the lead targets, with its most robust interaction occurring with GSK3β (1Q41), yielding a free binding energy of -55.13 kcal/mol. Similarly, quercetin showcased elevated complex stability across various lead targets, with its most favorable interaction occurring with the A2 receptor, resulting in a free binding energy score of -48.76 kcal/mol. Other hit ligands also demonstrated commendable complex stabilities with these lead targets.

Interestingly, the co-ligands also displayed favorable stability with their respective proteins, with the co-ligand in JNK2 registering the highest stability (free binding energy score of -124.04 kcal/mol) and the co-ligand in catechol-o-methyltransferase exhibiting the lowest stability (free binding energy score of -8.34

kcal/mol). Based on these calculations, it can be inferred that due to the consistent strong complex stability observed with ellagic acid and quercetin across all lead targets, these compounds may competitively induce prolonged and enhanced biological responses when compared to the co-ligands and other hits.

Molecular Interaction Profiles

Studies have revealed that the diversity in binding scores and affinities exhibited by the identified hit compounds within this study is attributed to their distinct interaction profiles with specific amino acid residues located at the binding sites of the lead target proteins (Owoloye et al., 2022; Ajiboye et al., 2023). These residues are pivotal contributors to the biological functionalities of these proteins. The visualization of intermolecular interactions between the hit ligands and the lead targets unveiled the establishment of crucial non-covalent bond types, which assume pivotal roles in shaping the structure and stability of the ligand-receptor complex. This intricate interplay of interactions underscores the foundation of a drug-receptor complex that governs the subsequent biological responses.

To gain insight into the mechanistic underpinnings of these interactions, the unique interactions of the hit compounds were compared with those of the co-crystallized ligands. This comparative analysis enabled the identification and delineation of the key amino acid residues situated at the binding sites of the proteins. These residues serve as focal points of interaction that orchestrate the binding process and influence the overall stability and specificity of ligand binding to the target proteins (Khazanov et al., 2013).

Catechol-O-methyltransferase

Figure 3a-e, displayed above, elucidates the distinct molecular interactions of the hit ligands with the catechol-O-methyltransferase (COMT) protein. The identification of the unique ligand occupying the catechol-binding site, known as the catalytic site, facilitated the identification of key amino acid residues forming this critical region. Drawing from visualization of docking simulations in conjunction with insights from published literature, the following amino acid residues, among others, have been recognized as vital constituents of the catalytic cavity: N170, M40, LYS144, E90, W143, and E199. These residues play pivotal roles in promoting inhibition, a novel avenue in the treatment of Parkinson's disease (PD), as studies have indicated (Rutherford et al., 2008).

The hit compounds exhibited a greater number of hydrogen bond interactions, with both ellagic acid and epicatechin forming five hydrogen bonds each. In comparison, the co-crystallized ligand formed only two hydrogen bonds. Notably, within quercetin, two hydroxyl groups on a phenyl group established hydrogen bond networks with E199 and N170, simultaneously engaging in a metal-ligand interaction with Mg2+, a co-factor known to facilitate the methylation process at the binding site of COMT (Rutherford et al., 2008). Similarly, ellagic acid's hydroxyl groups participated in three hydrogen bond networks with E199 and N170, along with a metal-ligand interaction with Mg2+. Moreover, one oxygen atom on a carbonyl

group and another on an oxa-cyclohexane group formed hydrogen bonds with adjacent water molecules within the binding pocket (as depicted in Figure 3b).

Figure 3c and 3d exhibit the interactions of Epicatechin and catechin, structurally akin compounds. Epicatechin formed five hydrogen bond interactions, while catechin formed four, both with E199 and N170. These interactions were facilitated by hydroxyl groups situated on their respective phenyl moieties. Additionally, both compounds engaged in non-covalent bonding with Mg2+. Notably, a distinctive feature of catechin's interaction involved a pi-pi bond with the hydrophobic W143. This interaction likely contributes to the higher binding score of catechin in comparison to epicatechin, which employed two of its hydroxyl groups to form conventional hydrogen bonds with surrounding water molecules.

It is imperative to acknowledge that the augmented binding affinities and complex stability potentially observed in ellagic acid, as compared to other hit compounds, might stem from its compact structural formula. This structure comprises moieties of phenyl and oxacyclohexanes linked through robust covalent C-C bonds. This structural characteristic potentially enhances its interaction capabilities with the catalytic site of COMT.

Dopamine-D1 Receptor

The interaction between the dopamine D1 receptor and the co-crystallized ligand, as visualized in Figure 4c, provides valuable insights into the amino acid residues contributing to the modulation of the D1 receptor at its orthosteric site. These residues have been corroborated by existing literature (Teng et al., 2022) and validated through the NCBI's conserved domain database. Notably, residues such as D103, F288, F289, F313, S198, and S107 play integral roles in this modulation process. Quercetin, through strategic utilization of two hydroxyl groups and the oxygen atom within its carbonyl group, establishes three hydrogen bond interactions with S198, D103, and S107. Notably, pi-pi stacking interactions are observed between the phenyl scaffolds of quercetin and the phenylalanine residues at positions 313 and 288 (F288 and F313). These multifaceted non-covalent interactions collectively contribute to the pronounced binding affinities demonstrated by quercetin towards the D1 receptor. Furthermore, the structural arrangement and interactions substantiate the stability of the drug-receptor complex formed. In contrast, ellagic acid engages in a solitary conventional hydrogen bond with S107, utilizing the oxygen atom substitution on one of its oxacyclohexane groups as the hydrogen bond acceptor. In tandem with this hydrogen bond, ellagic acid's phenyl and oxane scaffolds interact with hydrophobic phenylalanine residues (F288 and F289), leading to pi-pi stacking formations. Remarkably, ellagic acid's elevated docking scores and free binding energy can be attributed to the robust hydrophobic interactions, such as pi-pi bonds, sustained during the docking simulations, despite its comparatively fewer hydrogen bond formations in comparison to quercetin. The graphical depictions presented in the figures 4a-c serve as a comprehensive foundation for understanding the sustained higher affinities exhibited by our identified hit compounds in contrast to the co-crystallized ligand within the context of the D1 receptor. The co-crystallized ligand, in isolation, engages in merely three interactions, comprising two hydrogen bonds with D103 and a pi-pi bond with F289.

Collectively, these findings significantly contribute to the scientific discourse, elucidating the intricate interactions that underlie the elevated binding affinities of our hit compounds relative to the co-crystallized ligand within the dopamine D1 receptor framework.

Glycogen Synthase Kinase 3β

Research has highlighted the pivotal roles of certain hinge residues situated within the ATP binding site of GSK3B, specifically V135, E137, N200, C199, Q185, L188, and D133, in orchestrating the inhibition of GSK3B. This inhibition strategy has emerged as a prominent pharmacological approach for addressing neurological disorders and various other pathological conditions (Bertrand et al., 2003). Notably, the co-crystallized ligand demonstrates a remarkable binding affinity with GSK3B, potentially attributed to its adept utilization of the N1 and O2 atoms present within its pyrrolidine-2-one ring. These atoms engage in forming hydrogen bonds, with D133, which bears a negative charge, and hydrophobic V135, respectively. Additionally, a conventional hydrogen bond is established with a water molecule that, in turn, forms a hydrogen bond with the backbone Q185. This strategic interaction involving a bridging water molecule contributes to enhancing the stability of this binding interaction (as depicted in Figure 5d). Existing research has indicated that this bridging water molecule plays a critical role as a connecting link, fortifying the interaction between inhibitors and the Q185 residue (Bertrand et al., 2003).

Similarly, ellagic acid and quercetin exhibit analogous bridging interactions through water molecules within their intermolecular interactions with GSK3B. However, such bridging interaction is notably absent in the case of epicatechin (Figure 5c). Furthermore, ellagic acid and quercetin establish four and six hydrogen bonds, respectively, with GSK3B. Conversely, epicatechin showcases the least number of hydrogen bonds, numbering three (Figure 5a-c).

The insight into the distinct interactions of these hit compounds with GSK3B not only sheds light on their binding affinities but also unveils their structural and functional attributes within the inhibition process. These findings contribute significantly to the understanding of the intricate molecular dynamics driving the interactions of these compounds with GSK3B, advancing the broader discourse on the pharmacological manipulation of this target.

c-Jun N-terminal-Kinase 2

Mitogen-Activated Protein Kinases (MAPKs) have been extensively investigated for their central involvement in a multitude of pathways pivotal to inflammation and neurological diseases (Moens et al., 2013; Caliz et al., 2022). Over time, the development of inhibitors has been an active area of research, aimed at modulating the activity of this intriguing target. The current study seeks to identify efficacious inhibitors that hold promise for the treatment of PD. Illustrated in Figures 6a-e are the intricate molecular interactions between our hit ligands, the co-crystallized ligand, and the JNK2 protein. These interactions form the foundation for the observed disparities in binding affinities and the stability of the ligands-protein complex.

Remarkably, investigations have revealed that ligand binding within the ATP binding pocket of the JNK2 protein induces a conformational change, effectively hindering the activation of the phosphorylation activity associated with this novel target. The co-crystallized ligand serves as a guide for identifying key residues situated within this pocket. M111, D169, and E73 are notably mapped residues, and literature has indicated the presence of other residues such as I32, M108, and K55 that envelop this site (Kuglstatter et al., 2010).

The study's findings unveil robust molecular interactions between the co-crystallized ligand and several of these salient residues (as depicted in Figure 6a). This ligand forges six hydrogen bonds with M111, positioned at the hinge region, E73, a highly conserved residue, and D169, which contributes to the DFG-out conformation—a configuration conducive to JNK2 inhibition, as corroborated by studies (Duong et al., 2020). Epicatechin, meanwhile, establishes four hydrogen bonds with the aforementioned residues, facilitated by its hydroxyl groups. Additionally, epicatechin forms a hydrophobic bond with K55 through the creation of a pi-cation interaction. Similarly, quercetin establishes four hydrogen bonds, paralleling epicatechin's interactions. Catechin, in contrast, engages in both polar interactions (hydrogen bonds) and hydrophobic interactions (pi-pi stacking and pi-cation bonding) with the protein's residues. In comparison, ellagic acid forms only a single hydrogen bond, notably with the highly conserved E73. This limited molecular bonding potentially contributes to the comparatively lower binding free energy observed in the ellagic acid-JNK2 complex.

Adenosine A2 Receptor

Investigations have unveiled that the A2AR co-ligand engages closely with the residues comprising the protein's hydrophobic pocket. Residues such as F168, I274, L249, M270, W246, V84, and N253 collectively constitute the hydrophobic binding site of this protein (Doré et al., 2011). The co-ligand demonstrates a pi-stacking interaction with F168 and further forms a hydrogen bond with N253. These two interactions hold great significance, as highlighted by Doré et al. Our findings demonstrate the analogous interactions of the hit ligands with these residues. Each of the hit ligands establishes a minimum of two hydrogen bonds with these residues, with catechin displaying three hydrogen bonds. Furthermore, the hit ligands actively participate in pi-stacking interactions, a salient binding modality that has been extensively explored for its role in enhancing both the binding affinities and the overall stability of the protein-ligand complex (Pyrkov et al., 2009).

Phosphoinositide-3-Kinase

The inhibitory mechanisms exhibited by both the co-crystallized ligand and the hit ligands are intricately associated with the presence of specific amino acid residues situated within the binding site of phosphoinositide kinase 3 (PI3K), as well as the diverse types of bonds forged with these ligands (Certal et al., 2012). Remarkably, these ligands, including the distinct ligand binding to the same active site, demonstrated analogous activities, as evidenced by their binding scores (detailed in Table 2) derived from their interactions.

Analyzing the co-crystallized ligand and its distinctive interaction profile, it is apparent that this ligand establishes two hydrogen bonds and a single pi-pi stacking interaction. These interactions involve D964, V882, and Y867. The co-crystallized ligand effectively utilizes the oxygen substituent in its morpholine moiety, as well as the oxygen substitute in its pyrimidinone moiety and the pyrimidinone scaffold itself, to form these interactions (depicted in Figure 8a).

Ellagic acid, exhibiting the highest docking score, also shares analogous interaction patterns with the standard ligand. It manifests three distinct molecular interactions—two hydrogen bonds with K833 and V882 and one pi-stacking interaction with Y867. These interactions are facilitated through the hydroxyl groups present on ellagic acid's phenyl moieties and its oxacyclohexane group (illustrated in Figure 8c).

Quercetin, catechin, and epicatechin predominantly established varying numbers of hydrogen bonds with similar residues, including V882, D964, D950, K833, E880, Y867, and S806. Specifically, quercetin had the highest number of hydrogen bonds (as depicted in Figure 8e), while catechin displayed the fewest (shown in Figure 8b). These interactions collectively contribute to the distinctive inhibitory properties of each compound.

Sirtuin-2

Sirtuins have been extensively investigated for their fundamental roles in a myriad of cellular processes, and their dysregulation has been demonstrated to assume critical significance in the pathophysiology of diverse diseases, including PD (Liu et al., 2020; Rumpf et al., 2015). The present study was meticulously undertaken with the objective of identifying enduring and efficacious inhibitors targeting this novel protein.

The unique/co-ligand employed its NH-group to catalyze the formation of two hydrogen bonds, establishing intricate connections with L138 and G141. In parallel, catechin harnessed the hydroxyl groups embedded within its molecular framework, orchestrating a network of three hydrogen bonds. In contrast, both epicatechin and quercetin exhibited singular pi-stacking interactions, each interplaying with Y139 (Figure 9a-d).

The examined hit ligands exhibited a relatively restrained number of interactions with the sirtuin protein under scrutiny. This reduced interaction propensity potentially contributes to the observed lower complex stabilities—a parameter intrinsically linked to the binding free energy. Upon juxtaposition with the established standard (Table 2), these distinct patterns of interaction and stability collectively contribute to the nuanced attributes of the hit ligands compared to the reference ligand.

c-Jun N-terminal-Kinase 3

Figure 10a and 10b provide an intricate glimpse into the molecular interplay involving JNK3, the co-crystallized ligand, and the sole hit ligand (high binding affinity of -11.329kcal/mol), quercetin. A discernible observation is the distinctive formation of a greater number of hydrogen bonds by the unique ligand with both the protein and two adjacent water molecules. This interaction pattern, which has been

documented as a distinct binding mode exhibited by the unique ligand, significantly contributes to its inhibitory attributes, as corroborated by its binding score (detailed in Table 1) (Feng et al., 2021).

Concurrently, quercetin demonstrates robust and substantive molecular interactions with JNK3. Evidently, it establishes a total of three hydrogen bonds, involving M149, E147, and I70 residues. The underlying mechanism entails the strategic utilization of two hydroxyl groups, serving as hydrogen bond acceptors, in conjunction with an oxygen atom originating from its carbonyl group, which assumes the role of a hydrogen bond donor.

Pharmacokinetics Prediction

Following the meticulous evaluation of the potency and disparate affinities exhibited by these ligands, it becomes imperative to delve into their pharmacokinetic properties. This inquiry becomes indispensable to address concerns ranging from potential side effects and toxicity to challenges like limited absorption and inadequate clearance (Guengerich, 2011; Kola and Landis, 2004). These factors, often encountered during the drug development process, pose significant hurdles, leading to the attrition of a substantial number of promising compounds with therapeutic potential. This phenomenon underscores the paramount significance of investigating the pharmacokinetic attributes of hit compounds, a phase that serves as a pivotal bridge from preclinical investigation to clinical trials (Wishart, 2007; Ajiboye et al., 2021; Oyinloye et al., 2021).

Thus, in consonance with this imperative, our study embarked on a comprehensive exploration of the physicochemical profiles of quercetin, ellagic acid, epicatechin, and catechin. This exploration unfolded through a meticulous examination of their absorption, distribution, metabolism, excretion, and toxicity properties. Such an investigation, underpinned by a commitment to ensuring safety and optimal efficacy, forms a foundational step in navigating the complex landscape of drug development.

To conduct this assessment, we harnessed two distinct methodologies, leveraging the Qikprop plugin within Schrodinger Maestro and harnessing the capabilities of SwissADME (Daina et al., 2017). The outcome of these analyses encompassed a spectrum of descriptors, designed to gauge the drug-likeness and pharmacokinetic attributes inherent to our hit compounds. Parameters including molecular weight, the tally of hydrogen bond acceptors and donors, adherence to Lipinski's Rule of Five, and the potential for blood-brain barrier permeability stood at the forefront of these descriptors. This intricate web of characteristics synergistically provided an insightful depiction of the drug-like attributes of our compounds.

The culmination of these analyses serves to shed light on the structural and physicochemical attributes that shape the drug potential of our hit compounds. Such insights not only facilitate the formulation of compounds with an enhanced likelihood of translational success but also contribute to a holistic understanding of the broader pharmacological landscape.

The results, as succinctly presented in Table 3, offer profound insights into the diverse physicochemical properties of the hit ligands, a key determinant of their drug-likeness. Critical parameters such as the count of hydrogen bond acceptors and donors, molecular weight, and the octanol/water partition coefficient (QPlogPo/w) underwent thorough evaluation. Promisingly, the findings uniformly indicated that all hit ligands conform to the accepted ranges (as elaborated in the accompanying text below Table 3) for these physicochemical attributes, reaffirming their suitability for drug development.

Oral bioavailability, a pivotal facet of drug candidacy, was rigorously assessed utilizing Lipinski's Rule of Five, a well-established set of criteria employed to gauge the likelihood of compounds being administered orally (Lipinski et al., 2001). As delineated in the text below Table 3, it is posited that if a compound successfully satisfies at least three out of the five rules, it is deemed to possess favorable oral bioavailability. Notably, all hit ligands effortlessly met Lipinski's criteria, with only catechin and epicatechin exhibiting a minor deviation by violating a single criterion. This collective adherence underscores their oral bioavailability, a key consideration in their developmental potential.

Furthermore, these findings are fortified by the assessments of Human Oral Availability (HOA), which unequivocally indicate that the compounds possess medium to high oral availability. This signifies their enhanced propensity for absorption within the gastrointestinal tract (GIT), a pivotal attribute for potential oral drug administration. The pharmacokinetic attributes of the compounds were subjected to comprehensive scrutiny, encompassing evaluations of their binding to human serum albumin, potential blockage of HERG K+ channels, and blood-brain barrier permeability. Impressively, the values obtained for these parameters consistently fell within the recommended ranges (Table 3). While catechin and epicatechin exhibited slightly elevated scores for HERG K+ channel blockage, this minor pharmacokinetic discrepancy notwithstanding, the overall assessment underscores the excellent pharmacokinetic profiles of these compounds. Such profiles bode well for the efficient distribution of the compounds and their metabolites to the precise locations within the body, where they can exert their distinctive pharmacological significance.

The result presented in Table 4 further enriches our understanding of the hit ligands by delving into their potential toxic effects. Notably, the hit ligands exhibited no toxic indications of mutagenicity, tumorigenicity, or irritancy, except for quercetin, which displayed elevated tumorigenicity. This holistic evaluation enhances our comprehension of the compounds' safety profiles, an indispensable aspect in shaping their potential as viable therapeutic candidates.

In summation, these multifaceted analyses collectively validate the promising drug-like attributes and pharmacokinetic profiles of the hit ligands. These findings collectively fortify their potential as candidates for further development and eventual translation into effective therapeutic agents, poised to address the intricate challenges posed by diseases such as PD.

Density functional theory (DFT) is a computational approach that characterizes molecular systems based on electron density, rather than wavefunctions (Rong et al., 2020). In this study, we investigated the frontier molecular orbitals (FMOs), specifically the highest occupied molecular orbital (HOMO) and the

lowest unoccupied molecular orbital (LUMO), using DFT to explore the electronic structure and reactivity of various ligands. The HOMO represents the highest energy orbital occupied by electrons in a molecule's electronic configuration. It plays a crucial role in diverse chemical processes, such as ionization, electron transfer, and chemical reactions. On the other hand, the LUMO is the lowest energy orbital without any electrons, and its characteristics are significant in understanding molecular properties like electron affinity and reactivity towards electron acceptance. The optimized, HOMO, and LUMO structures are present in the supplementary file 2 (SF 2).

The DFT calculations provided optimized HOMO and LUMO regions for the four test compounds including the co-ligands, as shown in Figure 35 (Dorafshan et al., 2022). The computed HOMO energy values ranged from -5.47 to -5.30 eV, while the LUMO energy values ranged from -1.84 to -2.90 eV. Among the compounds, doramapimod exhibited the lowest HOMO energy (-5.06 eV), whereas dopamine had the highest LUMO energy (0.24 eV), as listed in Table 5. Additionally, we determined the band gap energy (Eg) for each compound, which ranged from 3.63 to 5.76 eV. Quercetin and dopamine displayed the lowest and highest Eg values, respectively. The band gap energy is an essential factor in drug development using DFT calculations (Park et al., 2016). A large band gap energy suggests low conductivity and reduced reactivity, making it less likely to interfere with other biological systems.

Conversely, a small band gap energy indicates higher conductivity and reactivity (Kessler et al., 2022; Olugbogi et al., 2023). Further investigations into compound stability and reactivity were performed by calculating global reactivity descriptors, including chemical hardness (η), softness (δ), electronegativity (χ), ionization potential (I), and electron affinity (A). These values were employed to gain insight into the ligands' stability and reactivity, as well as the stability of co-ligands, as presented in Table 5.

In summary, the HOMO energy (E_{HOMO}) indicates a molecule's capacity to donate electrons, while the LUMO energy (E_{LUMO}) predicts its ability to accept electrons. Higher E_{HOMO} values and lower E_{LUMO} values contribute to increased molecular reactivity. Our findings from this study highlight the test compounds' electron-donating capabilities based on their E_{HOMO} values and their ability to accept electrons based on their E_{LUMO} values. This knowledge is valuable for understanding the electronic properties and reactivity of the ligands examined in this investigation.

Molecular Dynamic Simulations (MDS)

Molecular dynamics simulations (MDS) are crucial in *in silico* studies for capturing the dynamic nature of biomolecular interactions (Vidal-Limon, et al., 2022; Olugbogi et al., 2023), where root-mean-square deviation (RMSD) provides insights into the stability of the system, and root-mean-square fluctuation (RMSF) offers details on the flexibility and movement of specific residues over time, both critical for understanding the function and behavior of molecular systems. In this current study, GSK3 Beta, identified as a promising target, along with the top-scoring ligands and a co-ligand, underwent MDS for a duration of 200 nanoseconds (ns).

The RMSD graph for the co-ligand (Figure 11 A) in complex with GSK3 beta over a 200 ns MDS shows the stability and dynamic behavior of both the protein (blue line) and ligand (red line). Observing the protein RMSD, it remains relatively constant with minor fluctuations for all test ligands including the co-ligand, indicating that the protein structure maintains its integrity throughout the simulation time. A stable protein RMSD is indicative of a reliable simulation and suggests that the protein did not undergo significant conformational changes, which is essential for valid drug-target interaction studies (Lecina et al., 2017; Olugbogi et al., 2023). The ligand RMSD, conversely, displays pronounced fluctuations, particularly with a sharp peak around 175 ns. This suggests that while the ligand generally maintains an interaction with the binding site, there are moments of significant conformational change or temporary loss of binding.

The consistent low-level fluctuations before this peak imply a stable interaction, but the spike could indicate transient unbinding or reorientation within the active site (Alade et al., 2023). Summarily, the co-ligand demonstrates a mostly stable interaction with GSK3 beta with occasional dynamic events. The stability for most of the simulation time suggests that the co-ligand could be a viable candidate for inhibiting GSK3 beta activity. However, the observed peak in ligand RMSD highlights the need for further investigation to understand the full nature of the interaction, and to assess the binding mode's potential impact on the efficacy and specificity of the co-ligand as a therapeutic agent.

Ellagic acid (Figure 11 B) in complex with GSK3 beta across a 200 ns MDS presents the stability and dynamics of the protein-ligand interaction. The ligand RMSD, (red line), shows more pronounced fluctuations, indicative of a dynamic interaction with the protein. The absence of extreme peaks suggests that ellagic acid maintains consistent contact with the protein's binding site, although with some degree of flexibility. This flexibility could be crucial for the ligand's ability to adapt to the shape of the binding pocket and form stable interactions (Amaral et al., 2017; Teilum et al., 2009). In a nutshell, the ellagic acid appears to maintain a stable interaction with the GSK3 beta protein throughout the simulation, with the expected dynamic behavior that could facilitate effective binding. These results suggest that ellagic acid is a promising candidate for further study as a potential inhibitor of GSK3 beta, with the potential for therapeutic application.

For the ligand quercetin (red line) in Figure 11 C, the RMSD displays a trend of moderate fluctuations, which implies a dynamic yet relatively stable interaction with GSK3 beta. There are no excessive peaks indicating major conformational shifts or dissociation events, suggesting that quercetin maintains consistent contact with the protein's active site. The RMSD profiles indicate that quercetin forms a stable complex with GSK3 beta, with both the protein and ligand demonstrating behavior conducive to a sustained interaction. This suggests that quercetin is a promising ligand for further investigation as a GSK3 beta inhibitor, with potential therapeutic implications (Jung et al., 2017).

The RMSD graph for epicatechin (Figure 11 D) in complex with GSK3 beta over a 200 ns MDS illustrates the dynamic interaction between the ligand and the protein. The blue line, representing the protein RMSD, shows a relatively stable profile with modest fluctuations. This indicates that the GSK3 beta protein

maintains its structural integrity throughout the simulation, which is desirable for a protein that could be targeted by drugs (Ruiz et al., 2022). On the other hand, the red line, indicating the ligand RMSD, exhibits considerable variability. The pronounced fluctuations suggest that epicatechin may have multiple binding conformations or that it experiences flexible interactions with the protein's binding site. This could mean that the ligand is sampling various poses or that it is loosely bound, which may affect the strength and specificity of its inhibitory action. This data suggests that while the GSK3 beta protein remains stable, epicatechin interacts dynamically with the protein. While such flexibility can sometimes be advantageous, allowing the ligand to adapt to different protein conformations, it may also result in reduced binding affinity (Seo et al., 2014). To draw a definitive conclusion on the therapeutic potential of epicatechin as a GSK3 beta inhibitor, further analysis would be required, including experimental validation to corroborate the in-silico findings.

Based on the RMSD analysis of the four complexes, co-ligand, ellagic acid, quercetin, and epicatechin in complex with GSK3 beta over a 200 ns MDS, quercetin emerges as the most promising candidate. It demonstrates a notably stable interaction profile, indicated by minimal fluctuations in RMSD values, which suggests a strong and consistent binding affinity to the protein. This stability is a crucial indicator of the potential efficacy of quercetin as a GSK3 beta inhibitor, making it a compelling molecule for further drug development and pharmacological studies., as validated in other studies (Islam et al., 2021). The other compounds, while showing varying degrees of interaction dynamics, did not exhibit the same level of consistent stability as quercetin, underscoring its superiority among the tested ligands in the context of this simulation.

The Root Mean Square Fluctuation (RMSF) plot for the GSK3 beta protein in complex with ligands over a 200 ns MDS provides insights into the flexibility and dynamics of individual amino acid residues upon ligand binding.

The RMSF values, plotted against the residue index, exhibit peaks that correspond to regions of the protein with higher flexibility (Ghahremanian et al., 2022). Lower RMSF values indicate more rigid, less fluctuating regions, often associated with the core structural elements of the protein. In contrast, higher RMSF values point to flexible loops or termini that may be involved in ligand binding or protein-protein interactions (Rahban et al., 2022). In this simulation (Figure 12 A), the observed peaks suggest that certain residues of GSK3 beta exhibit considerable flexibility, which could be critical for the protein's functional conformational changes upon ligand binding. These flexible regions may facilitate the accommodation of different ligands within the binding site, allowing for induced-fit interactions that are essential for effective inhibition. Lastly, the RMSF analysis of GSK3 beta reveals distinct regions of flexibility that may play a significant role in ligand binding and the protein's biological function.

Upon binding with ellagic acid (Figure 12 B), the GSK3 beta protein shows an overall moderate level of flexibility across its structure, with certain residues exhibiting significant fluctuations. These specific areas of heightened flexibility might be crucial for the accommodation of the ellagic acid molecule and could be indicative of allosteric sites or regions that undergo conformational changes upon ligand

binding (Glasgow et al., 2023). In sum, the RMSF analysis indicates that while GSK3 beta maintains a stable structure overall when bound to ellagic acid, there are flexible regions that could be important for the protein's interaction with the ligand. Understanding these fluctuations is essential for elucidating the binding mechanism of ellagic acid and its potential impact on the protein's function, which can inform the design of targeted therapeutic strategies (Singh et al., 2016).

The plot reveals varying degrees of residue mobility along the protein chain as displayed in Figure 12 C. In the presence of quercetin, the GSK3 beta protein exhibits specific regions of heightened mobility, which may correspond to the binding site or adjacent areas that undergo conformational changes to accommodate the ligand. This dynamic behavior is essential for the protein's biological function and could be leveraged to design more effective GSK3 beta inhibitors (Cohen et al., 2004). In the end, the interaction with quercetin appears to preserve the overall structural integrity of GSK3 beta while permitting necessary flexibility at key residues. This balance between stability and mobility is characteristic of effective ligand binding and positions quercetin as a promising candidate for further therapeutic exploration in targeting GSK3 beta.

In this case (Figure 12 D), the binding of epicatechin to GSK3 beta appears to preserve the overall structural framework while allowing for necessary mobility in key regions, which may facilitate epicatechin's interaction with the active site and potentially affect the protein's activity. The presence of both stable and flexible regions upon ligand binding is a positive indication of a well-behaved protein-ligand complex (Majewski et al., 2019). By and large, we can say, the interaction with epicatechin demonstrates that while GSK3 beta retains a stable conformation overall, certain residues exhibit the flexibility needed for functional activity. This balance is crucial for the development of effective therapeutic agents, and the RMSF data suggests that epicatechin could be a suitable candidate for further drug development efforts targeting GSK3 beta.

The RMSF analyses of GSK3 beta with the four ligands (co-ligand, ellagic acid, quercetin, and epicatechin) over a 200 ns MDS reveal that quercetin exhibits the most favorable profile, with balanced flexibility that suggests efficient ligand accommodation without compromising the protein's structural integrity. Compared to the RMSD results, which also indicated quercetin's complex as having the most stable ligand-protein interaction, the RMSF findings corroborate this by showing an optimal range of residue fluctuations essential for functional activity. This synergy between RMSD and RMSF outcomes for quercetin highlights its potential as the most promising candidate for further investigation, underscoring the ligand's ability to maintain a stable binding while allowing the necessary protein dynamics for biological activity.

The Protein-Ligand interaction histogram illustrates the interaction profile of all three test ligands and the co-ligand (Figure 13) with various residues of a protein (Beura et al., 2020). Notably, the green bars, representing hydrogen bonds, are predominantly associated with D133 and V135 residues in Figure 13 A, suggesting strong and specific interactions that are key for ligand binding stability. Similarly, these contacts with V135 and D133 were initially reported post XP-docking. The ash-grey bars indicating

hydrophobic interactions, although more distributed, show a significant interaction at L132, which could contribute to the hydrophobic core of the binding pocket and thus enhance the ligand's affinity. The blue bars, denoting water bridges, suggest that solvent-mediated interactions might play a role in the binding mechanism, as seen with V135, potentially impacting the ligand orientation and possibly its dynamism within the active site. The presence of red bars for ionic bonding is absent, indicating that electrostatic interactions are not a significant contributor to binding in this context.

The length of the bars corresponds to the interaction fraction, with longer bars indicating more prevalent contact throughout the simulation. The strong hydrogen bonding at D133 and V135, combined with hydrophobic contacts at L132, point to these residues as critical for ligand binding. This interaction mapping provides a clear indication that the binding of the co-ligand to the protein is characterized by a balance of hydrogen bonds and hydrophobic interactions. The interactions with D133 and V135 appear to be key for the stability of the ligand within the protein’s binding site, making these residues potential targets for enhancing ligand affinity and specificity in drug design.

The interaction mapping of ellagic acid (Figure 13 B) with various amino acids in the protein structure reveals a diverse interaction profile. Hydrogen bonds, depicted in green, appear to be the second most prevalent and significantly involved with certain residues like V135 for 50%, D133 and K85 for more than 70% of the simulation time, suggesting that these interactions are likely critical for the stability and specificity of ellagic acid within the binding site. These types of hydrogen bonds were also seen during the initial docking analysis. Hydrophobic interactions, shown in ash-grey, are less frequent but present, with a notable interaction at L188 (50% simulation time). This indicates a contribution to the non-polar interaction landscape that supports ligand binding affinity.

The blue bars which are the most prevalent, representing water bridges, suggest the involvement of solvent molecules in stabilizing the ligand-protein complex, possibly affecting ligand positioning and dynamics with I62, N64, L85, D133, V135, and D200 involved in more than 70% of the simulation time. The presence of ionic interactions, marked in red, is minimal, suggesting that they do not play a significant role in the binding of ellagic acid to this protein. As a matter of fact, the interaction map suggests that ellagic acid binds to the protein with a strong reliance on hydrophobic interactions and a supportive role of hydrogen bonds, while ionic interactions and water bridges contribute less to the overall binding stability. The key residues involved in these interactions, particularly D133 and K85, may be critical targets for optimizing ligand binding and enhancing drug efficacy.

The interaction mapping for quercetin (Figure 13 C) with various amino acids at the active site of GSK3 beta illustrates a robust interaction profile, pivotal for stabilizing the ligand within the protein's binding site. The prevalence of hydrogen bonds, indicated in green, particularly with residues like D133, E97, and V135 for more than 79% of the simulation trajectory, emphasizes their crucial role in anchoring quercetin firmly within the binding pocket. Surprisingly, V135 was earlier reported in the docking study making the residue a key component for the binding of quercetin to GSK3B. These hydrogen bonds, due to their

length on the plot, suggest a strong and stable interaction. Hydrophobic contacts, shown in ash-grey, in this case are not significantly involved.

Water bridges on the other hand, depicted in blue, while present, constitute a major fraction of the interaction spectrum, suggesting a primary role in ligand stabilization (Matricon et al., 2020). It was seen in contact with E97, V135, D200, and N64 for 50% or more of the simulation trajectory. Ionic bonds, in red, had no impact on the binding. However, their presence indicates an intricate network of interactions involving the solvent, which may influence ligand dynamics and conformational flexibility (Wade et al., 1998). In all, quercetin exhibits a strong binding affinity for the GSK3B protein primarily through sustained hydrogen bonding and complementary hydrophobic interactions. The interaction map underscores the importance of key residues, especially D133, E97, and V135, which could be critical targets for enhancing ligand specificity and potency through drug design optimizations.

The interaction profile of epicatechin with GSK3B protein reveals a diverse and complex binding landscape (Figure 13 D). The histogram indicates the presence of hydrogen bonds, as shown in green, suggesting that epicatechin forms several key interactions, particularly with residues like D133 which was involved in the reported hydrogen bonds in Figure 5c and D200 for more than 60% of the simulation time, which contribute to the specificity and stability of the ligand within the binding site. The presence of hydrophobic interactions, denoted in ash-grey, although less dominant than hydrogen bonds, suggests that residues such as I62 and L188 contribute to the ligand's binding affinity through these interactions, possibly stabilizing the ligand in a defined conformation.

Notably, water bridges for N200 were seen for about 150% and D133 for about 80% of the simulation time, respectively. Ionic bonds are less prevalent but indicate the participation of the surrounding solvent in mediating interactions between epicatechin and the protein. In sum, the protein-ligand interaction mapping of epicatechin indicates a strong hydrogen bond network, complemented by essential hydrophobic contacts and additional interactions facilitated by water molecules and charge-charge interactions. This multifaceted interaction pattern underlines the complexity of the binding mechanism and could be insightful for the design of more potent derivatives or competitive inhibitors targeting GSK3B.

Conclusion

Parkinson’s disease is characterized by degeneration of the neurons caused by neuro-inflammation and oxidative stress. This study investigated the therapeutic effect of *Spondias mombin* against 35 PD-associated target proteins using in silico experiments. Quercetin, catechin, epicatechin, and ellagic acid are the major *Spondias mombin* compounds with high affinity for the PD-associated target proteins. These best ligands were also screened using MD simulations against GSK3 beta which emerged as the best target protein. The RMSD and RMSF report suggests quercetin as our best bet. The DFT results showed that the hit compounds have small band gap energy which indicates higher conductivity and

reactivity. Interestingly, the results demonstrate that *Spondias mombin* may represent a key bio-resource for the development of cheap PD drugs.

Abbreviations

PD
Parkinson's disease
DFT
Density Functional Theory
FMO
frontier molecular orbital
MDS
Molecular Dynamic Simulations
ADMET
Adsorption Distribution Metabolism Excretion and Toxicity
MM/GBSA
Molecular Mechanics/Generalized Born Surface Area

Declarations

Acknowledgment

We appreciate the entire Eureka Research Laboratory Team for their assistance during the review of this project.

Disclosure statement

The authors of this manuscript declared no conflict of interest.

Funding

The authors received no financial support for this manuscript's research, authorship, and/or publication.

Authors' Contributions

Conceptualization and Validation of results: O.A.J, A.O.L, S.E.O, and E.A.O.

Software and Formal analysis: E.A.O and A.O.L.

Data curation: S.E.O, and E.A.O.

Writing-original draft preparation: A.O.L, S.E.O, and E.A.O.

Writing-review and Editing: All authors partook in the manuscript writing, review and editing.

All authors read and approved the final manuscript for publication.

References

1. Abraham Vidal-Limon, José E. Aguilar-Toalá, and Andrea M. Liceaga, Journal of Agricultural and Food Chemistry 2022 70 (4), 934-943 DOI: 10.1021/acs.jafc.1c06110
2. Ajiboye, T.M. Fagbola, I.M. Folorunso, A.W. Salami, O.N. Aletile, B.A. Akomolede, F.I. Ayemoni, K.I. Akinfemiwa, V.O. Anwo, M.I. Ojeleke, B.E. Oyinloye, In silico identification of chemical compounds in Spondias mombin targeting aldose reductase and glycogen synthase kinase 3β to abate diabetes mellitus, Informatics in Medicine Unlocked, Volume 36, 2023, 101126, ISSN 2352-9148,https://doi.org/10.1016/j.imu.2022.101126.
3. Alade, A. A., Ahmed, S. A., Mujwar, S., Kikiowo, B., Akinnusi, P. A., Olubode, S. O., ... & Ohilebo, A. A. (2023). Identification of levomenthol derivatives as potential dipeptidyl peptidase-4 inhibitors: a comparative study with gliptins. Journal of Biomolecular Structure and Dynamics, 1-19.
4. Amaral, M., Kokh, D.B., Bomke, J. et al. Protein conformational flexibility modulates kinetics and thermodynamics of drug binding. Nat Commun 8, 2276 (2017). https://doi.org/10.1038/s41467-017-02258-w
5. Arciniegas Ruiz, S. M., & Eldar-Finkelman, H. (2022). Glycogen Synthase Kinase-3 Inhibitors: Preclinical and Clinical Focus on CNS-A Decade Onward. Frontiers in molecular neuroscience, 14, 792364. https://doi.org/10.3389/fnmol.2021.792364
6. Asiimwe, S., Anywar, G. U., Kakudidi, E. K., & Tugume, P. (2021). Medicinal Plants in Uganda as Potential Therapeutics against Neurological Disorders. Medicinal Herbs and Fungi: Neurotoxicity vs. Neuroprotection, 421-443.
7. Baig, M. H., Ahmad, K., Rabbani, G., Danishuddin, M., & Choi, I. (2018). Computer Aided Drug Design and its Application to the Development of Potential Drugs for Neurodegenerative Disorders. Current neuropharmacology, 16(6), 740–748. https://doi.org/10.2174/1570159X15666171016163510
8. Bandres-Ciga, S., Diez-Fairen, M., Kim, J. J., & Singleton, A. B. (2020). Genetics of Parkinson's disease: An introspection of its journey towards precision medicine. Neurobiology of disease, 137, 104782. https://doi.org/10.1016/j.nbd.2020.104782
9. Banerjee, P., Eckert, A. O., Schrey, A. K., & Preissner, R. (2018). ProTox-II: a webserver for the prediction of toxicity of chemicals. Nucleic acids research, 46(W1), W257–W263. https://doi.org/10.1093/nar/gky318
10. Bertrand, J. A., Thieffine, S., Vulpetti, A., Cristiani, C., Valsasina, B., Knapp, S., Kalisz, H. M., & Flocco, M. (2003). Structural characterization of the GSK-3beta active site using selective and non-selective ATP-mimetic inhibitors. Journal of molecular biology, 333(2), 393–407. https://doi.org/10.1016/j.jmb.2003.08.031
11. Beura, Satyajit & Prabhakar, Ch. (2020). In-silico strategies for probing chloroquine based inhibitors against SARS-CoV-2. Journal of Biomolecular Structure and Dynamics. 39. 1-25.

10.1080/07391102.2020.1772111.

12. Bohush, Anastasiia & Niewiadomska, Grazyna & Filipek, Anna. (2018). Role of Mitogen Activated Protein Kinase Signaling in Parkinson's Disease. International Journal of Molecular Sciences. 19. 2973. 10.3390/ijms19102973.
13. Borkotoky, Subhomoi & Meena, Chetan & Murali, Ayaluru. (2016). Interaction Analysis of T7 RNA Polymerase with Heparin and Its Low Molecular Weight Derivatives – An In Silico Approach. Bioinformatics and Biology Insights. 2016. 155. 10.4137/BBI.S40427.
14. Bowers, K.J., Chow, E., Xu, H., Dror, R.O., Eastwood, M.P., Gregersen, B.A., Klepeis, J.L., Kolossvary, I., Moraes, M.A., Sacerdoti, F.D., Salmon, J.K., Shan, Y., Shaw, D.E. (2006). "Scalable Algorithms for Molecular Dynamics Simulations on Commodity Clusters." Proceedings of the ACM/IEEE Conference on Supercomputing (SC06), Tampa, Florida, November 11-17.
15. Butcher, E. C., Berg, E. L., & Kunkel, E. J. (2004). Systems biology in drug discovery. Nature biotechnology, 22(10), 1253-1259.
16. Caliz, A. D., Vertii, A., Fisch, V., Yoon, S., Yoo, H. J., Keaney, J. F., Jr, & Kant, S. (2022). Mitogen-activated protein kinase kinase 7 in inflammatory, cancer, and neurological diseases. Frontiers in cell and developmental biology, 10, 979673. https://doi.org/10.3389/fcell.2022.979673
17. Castillo, V. & Onate, Maritza & Woehlbier, Ute & Rozas, Pablo & Andreu, Catherine & Medinas, Danilo & Valdés, P. & Osorio, Fabiola & Mercado, Gabriela & Vidal, René & Kerr, Bredford & Court, Felipe & Hetz, C.. (2015). Erratum: Functional role of the disulfide isomerse ERp57 in axonal regeneration (PLoS ONE (2015) 10:9 (e0136620) DOI:10.1371/journal.pone.0136620). 10. 10.1371/journal.pone.0140200.
18. Certal, V., Halley, F., Virone-Oddos, A., Thompson, F., Filoche-Rommé, B., El-Ahmad, Y., Carry, J. C., Delorme, C., Karlsson, A., Abecassis, P. Y., Vincent, L., Bonnevaux, H., Nicolas, J. P., Morales, R., Michot, N., Vade, I., Louboutin, A., Perron, S., Doerflinger, G., Tric, B., … Schio, L. (2012). Preparation and optimization of new 4-(morpholin-4-yl)-(6-oxo-1,6-dihydropyrimidin-2-yl)amide derivatives as PI3Kβ inhibitors. Bioorganic & medicinal chemistry letters, 22(20), 6381–6384. https://doi.org/10.1016/j.bmcl.2012.08.072
19. Chao Lu, Chuanjie Wu, Delaram Ghoreishi, Wei Chen, Lingle Wang, Wolfgang Damm, Gregory A. Ross, Markus K. Dahlgren, Ellery Russell, Christopher D. Von Bargen, Robert Abel, Richard A. Friesner, and Edward D. Harder Journal of Chemical Theory and Computation 2021 17 (7), 4291-4300 DOI: 10.1021/acs.jctc.1c00302
20. Cohen, P., Goedert, M. GSK3 inhibitors: development and therapeutic potential. Nat Rev Drug Discov 3, 479–487 (2004). https://doi.org/10.1038/nrd1415
21. Daina, A., Michielin, O. & Zoete, V. SwissADME: a free web tool to evaluate pharmacokinetics, drug-likeness and medicinal chemistry friendliness of small molecules. *Sci Rep***7**, 42717 (2017). https://doi.org/10.1038/srep42717
22. Daina, A., Michielin, O., & Zoete, V. (2017). SwissADME: a free web tool to evaluate pharmacokinetics, drug-likeness and medicinal chemistry friendliness of small molecules. Scientific reports, 7, 42717.

https://doi.org/10.1038/srep42717

23. Dolgacheva, Lyudmila & Berezhnov, Alexey & Fedotova, Evgeniya & Zinchenko, Valery & Abramov, Andrey. (2019). Role of DJ-1 in the mechanism of pathogenesis of Parkinson's disease. Journal of Bioenergetics and Biomembranes. 51. 10.1007/s10863-019-09798-4.
24. Dorafshan Tabatabai, A. S., Dehghanian, E., & Mansouri-Torshizi, H. (2022). In-silico and in-detail experimental interaction studies of new antitumor Zn (II) complex with CT-DNA and serum albumin. Journal of Biomolecular Structure and Dynamics, 1-18.
25. Doré, A. S., Robertson, N., Errey, J. C., Ng, I., Hollenstein, K., Tehan, B., Hurrell, E., Bennett, K., Congreve, M., Magnani, F., Tate, C. G., Weir, M., & Marshall, F. H. (2011). Structure of the adenosine A(2A) receptor in complex with ZM241385 and the xanthines XAC and caffeine. Structure (London, England : 1993), 19(9), 1283–1293. https://doi.org/10.1016/j.str.2011.06.014
26. druggability. J Chem Info Mod 49(2):377–389
27. Duong, M. T. H., Lee, J. H., & Ahn, H. C. (2020). C-Jun N-terminal kinase inhibitors: Structural insight into kinase-inhibitor complexes. Computational and structural biotechnology journal, 18, 1440–1457. https://doi.org/10.1016/j.csbj.2020.06.013
28. Ekor M. (2014). The growing use of herbal medicines: issues relating to adverse reactions and challenges in monitoring safety. Frontiers in pharmacology, 4, 177. https://doi.org/10.3389/fphar.2013.00177
29. Elbaz, Alexis & Levecque, Clotilde & Clavel, Jacqueline & Vidal, Jean-Sébastien & Richard, Florence & Amouyel, Philippe & Alpérovitch, Annick & Chartier-Harlin, Marie-Christine & Tzourio, Christophe. (2004). CYP2D6 Polymorphism, Pesticide Exposure, and Parkinson's Disease. Annals of neurology. 55. 430-4. 10.1002/ana.20051.
30. Feng, Y., Park, H., Ryu, J. C., & Yoon, S. O. (2021). N-Aromatic-Substituted Indazole Derivatives as Brain-Penetrant and Orally Bioavailable JNK3 Inhibitors. ACS medicinal chemistry letters, 12(10), 1546–1552. https://doi.org/10.1021/acsmedchemlett.1c00334
31. GAO, Lin A Thesis Submitted in Partial Fulfillment of the Requirements for the Degree of Doctor of Philosophy in Biomedical Sciences The Chinese University of Hong Kong August 2020
32. Ghahremanian, S., Rashidi, M. M., Raeisi, K., & Toghraie, D. (2022). Molecular dynamics simulation approach for discovering potential inhibitors against SARS-CoV-2: A structural review. Journal of molecular liquids, 354, 118901. https://doi.org/10.1016/j.molliq.2022.118901
33. Glasgow, A., Hobbs, H.T., Perry, Z.R. et al. Ligand-specific changes in conformational flexibility mediate long-range allostery in the lac repressor. Nat Commun 14, 1179 (2023). https://doi.org/10.1038/s41467-023-36798-1
34. Guengerich F. P. (2011). Mechanisms of drug toxicity and relevance to pharmaceutical development. Drug metabolism and pharmacokinetics, 26(1), 3–14. https://doi.org/10.2133/dmpk.dmpk-10-rv-062
35. Halgren TA (2009) Identifying and characterizing binding sites and assessing https://www.ncbi.nlm.nih.gov/cdd

36. Ishan Patro, Pankaj Seth, Nisha Patro, Prakash Narain Tandon The Biology of Glial Cells: Recent Advances, 2022
37. Islam, M. S., Quispe, C., Hossain, R., Islam, M. T., Al-Harrasi, A., Al-Rawahi, A., Martorell, M., Mamurova, A., Seilkhan, A., Altybaeva, N., Abdullayeva, B., Docea, A. O., Calina, D., & Sharifi-Rad, J. (2021). Neuropharmacological Effects of Quercetin: A Literature-Based Review. Frontiers in pharmacology, 12, 665031. https://doi.org/10.3389/fphar.2021.665031
38. Jha, Saurabh & Jha, Niraj & Kar, Rohan & Ambasta, Rashmi & Kumar, Pravir. (2015). p38 MAPK and PI3K/AKT signalling cascades in Parkinson's disease. International Journal of Molecular and Cellular Medicine. 4. 1-20.
39. Jung, Y., Shin, S.Y., Lee, Y.H. et al. Flavones with inhibitory effects on glycogen synthase kinase 3β. Appl Biol Chem 60, 227–232 (2017). https://doi.org/10.1007/s13765-017-0271-2
40. Kessler, A., Hedberg, J., Blomberg, E., & Odnevall, I. (2022). Reactive oxygen species formed by metal and metal oxide nanoparticles in physiological media—a review of reactions of importance to nanotoxicity and proposal for categorization. Nanomaterials, 12(11), 1922.
41. Khazanov, N. A., & Carlson, H. A. (2013). Exploring the composition of protein-ligand binding sites on a large scale. PLoS computational biology, 9(11), e1003321. https://doi.org/10.1371/journal.pcbi.1003321
42. Kola, I., & Landis, J. (2004). Can the pharmaceutical industry reduce attrition rates?. Nature reviews. Drug discovery, 3(8), 711–715. https://doi.org/10.1038/nrd1470
43. Kuglstatter, A., Ghate, M., Tsing, S., Villaseñor, A. G., Shaw, D., Barnett, J. W., & Browner, M. F. (2010). X-ray crystal structure of JNK2 complexed with the p38alpha inhibitor BIRB796: insights into the rational design of DFG-out binding MAP kinase inhibitors. Bioorganic & medicinal chemistry letters, 20(17), 5217–5220. https://doi.org/10.1016/j.bmcl.2010.06.157
44. Lecina, D., Gilabert, J.F. & Guallar, V. Adaptive simulations, towards interactive protein-ligand modeling. Sci Rep 7, 8466 (2017). https://doi.org/10.1038/s41598-017-08445-5
45. Lipinski CA, Lombardo F, Dominy BW, Feeney PJ. Experimental and computational approaches to estimate solubility and permeability in drug discovery and development settings. Adv Drug Deliv Rev 2001;46(1–3):3–26
46. Liu, Y., Zhang, Y., Zhu, K., Chi, S., Wang, C., & Xie, A. (2020). Emerging Role of Sirtuin 2 in Parkinson's Disease. Frontiers in aging neuroscience, 11, 372. https://doi.org/10.3389/fnagi.2019.00372
47. Majewski, M., Ruiz-Carmona, S. & Barril, X. An investigation of structural stability in protein-ligand complexes reveals the balance between order and disorder. Commun Chem 2, 110 (2019). https://doi.org/10.1038/s42004-019-0205-5
48. Matricon, P., Suresh, R. R., Gao, Z. G., Panel, N., Jacobson, K. A., & Carlsson, J. (2020). Ligand design by targeting a binding site water. Chemical science, 12(3), 960–968. https://doi.org/10.1039/d0sc04938g
49. Moens, U., Kostenko, S., & Sveinbjørnsson, B. (2013). The Role of Mitogen-Activated Protein Kinase-Activated Protein Kinases (MAPKAPKs) in Inflammation. Genes, 4(2), 101–133.

https://doi.org/10.3390/genes4020101

50. Mohamed, Asmaa & Abdel-Fattah, Dina & Abdel-Aleem, Ghada & El-Sheikh, Thanaa & Elbatch, Manal. (2023). Biochemical study of the effect of mesenchymal stem cells-derived exosome versus L-Dopa in experimentally induced Parkinson's disease in rats. Molecular and Cellular Biochemistry. 1-17. 10.1007/s11010-023-04700-8.
51. Nouri, P., Götz, S., Rauser, B., Irmler, M., Peng, C., Trümbach, D., Kempny, C., Lechermeier, C. G., Bryniok, A., Dlugos, A., Euchner, E., Beckers, J., Brodski, C., Klümper, C., Wurst, W., & Prakash, N. (2020). Dose-Dependent and Subset-Specific Regulation of Midbrain Dopaminergic Neuron Differentiation by LEF1-Mediated WNT1/b-Catenin Signaling. *Frontiers in cell and developmental biology*, *8*, 587778. https://doi.org/10.3389/fcell.2020.587778
52. Obodozie, O. O., Ameh, S. J., Afolabi, E. K., Oyedele, E. O., Ache, T. A., Onanuga, C. E., Ibe, M. C., & Inyang, U. S. (2010). A normative study of the components of niprisan–an herbal medicine for sickle cell anemia. Journal of dietary supplements, 7(1), 21–30. https://doi.org/10.3109/19390210903534988
53. Olugbogi EA, Omotuyi OI, Mesileya KT, Bodun DS, Omoseeye SD, Onoriode AO, Oluwamoroti FO, Adedara JF, Oriyomi IA, Bello FO, Olowoyeye FO, Laoye OG, Adebowale DB, Adebisi AD, Ogologo MC, Etukokwu OC, Onyemaobi IO, Jibril SY and Onyeka PC: Computer based screening of the anticancer property of selected panax ginseng phyto-ligands. Int J Pharm Sci & Res 2023; 14(4): 1714-27. doi: 10.13040/IJPSR.0975-8232.14(4).1714-27.
54. Olugbogi, E. A., Arobadade, O. A., Bodun, D. S., Omoseeye, S. D., Omirin, E. S., Fapohunda, O., ... & Omotuyi, O. I. (2023). Identification of apposite antagonist for androgen receptor in prostate cancer: an in-silico study of fenugreek compounds. Journal of Biomolecular Structure and Dynamics, 1-17.
55. Omotuyi, I. O., Nash, O., Ajiboye, B. O., Olumekun, V. O., Oyinloye, B. E., Osuntokun, O. T., Olonisakin, A., Ajayi, A. O., Olusanya, O., Akomolafe, F. S., & Adelakun, N. (2021). Aframomum melegueta secondary metabolites exhibit polypharmacology against SARS-CoV-2 drug targets: in vitro validation of furin inhibition. Phytotherapy research: PTR, 35(2), 908–919. https://doi.org/10.1002/ptr.6843
56. Owoloye AJ, Ligali FC, Enejoh OA, Musa AZ, Aina O, Idowu ET, et al. (2022) Molecular docking, simulation and binding free energy analysis of small molecules as PfHT1 inhibitors. PLoS ONE 17(8): e0268269. https://doi.org/10.1371/journal.pone.0268269
57. Oyinloye BE, Iwaloye O, Ajiboye BO. Polypharmacology of Gongronema latifolium leaf secondary metabolites against protein kinases implicated in Parkinson's disease and Alzheimer's disease. Scientific African 2021;12(3):e00826. https://doi.org/10.1016/j.sciaf.2021.e00826.
58. Poewe, W., Seppi, K., Tanner, C. M., Halliday, G. M., Brundin, P., Volkmann, J., Schrag, A. E., & Lang, A. E. (2017). Parkinson disease. Nature reviews. Disease primers, 3, 17013. https://doi.org/10.1038/nrdp.2017.13
59. Pyrkov, T. V., Pyrkova, D. V., Balitskaya, E. D., & Efremov, R. G. (2009). The role of stacking interactions in complexes of proteins with adenine and Guanine fragments of ligands. Acta naturae, 1(1), 124–

127.

60. Rahban, M., Zolghadri, S., Salehi, N., Ahmad, F., Haertlé, T., Rezaei-Ghaleh, N., Sawyer, L., & Saboury, A. A. (2022). Thermal stability enhancement: Fundamental concepts of protein engineering strategies to manipulate the flexible structure. International journal of biological macromolecules, 214, 642–654. https://doi.org/10.1016/j.ijbiomac.2022.06.154
61. Repici, Mariaelena & Giorgini, Flaviano. (2019). DJ-1 in Parkinson's Disease: Clinical Insights and Therapeutic Perspectives. Journal of Clinical Medicine. 8. 1377. 10.3390/jcm8091377.
62. Rong, C., Wang, B., Zhao, D., & Liu, S. (2020). Information-theoretic approach in density functional theory and its recent applications to chemical problems. Wiley Interdisciplinary Reviews: Computational Molecular Science, 10(4), e1461.
63. Rui, Wenjuan & Li, Sheng & Xiao, Hong & Xiao, Ming & Shi, Jingping. (2020). Baicalein Attenuates Neuroinflammation by Inhibiting NLRP3/caspase-1/GSDMD Pathway in MPTP Induced Mice Model of Parkinson's Disease. The international journal of neuropsychopharmacology. 23. 10.1093/ijnp/pyaa060.
64. Rumpf, T., Gerhardt, S., Einsle, O., & Jung, M. (2015). Seeding for sirtuins: microseed matrix seeding to obtain crystals of human Sirt3 and Sirt2 suitable for soaking. Acta crystallographica. Section F, Structural biology communications, 71(Pt 12), 1498–1510. https://doi.org/10.1107/S2053230X15019986
65. Rutherford, K., Le Trong, I., Stenkamp, R. E., & Parson, W. W. (2008). Crystal structures of human 108V and 108M catechol O-methyltransferase. Journal of molecular biology, 380(1), 120–130. https://doi.org/10.1016/j.jmb.2008.04.040
66. Salman, M. M., Al-Obaidi, Z., Kitchen, P., Loreto, A., Bill, R. M., & Wade-Martins, R. (2021). Advances in Applying Computer-Aided Drug Design for Neurodegenerative Diseases. International journal of molecular sciences, 22(9), 4688. https://doi.org/10.3390/ijms22094688
67. Sander, T., Freyss, J., von Korff, M., & Rufener, C. (2015). DataWarrior: an open-source program for chemistry aware data visualization and analysis. *Journal of chemical information and modeling*, *55*(2), 460–473. https://doi.org/10.1021/ci500588j
68. Sastry, G. M., Adzhigirey, M., Day, T., Annabhimoju, R., & Sherman, W. (2013). Protein and ligand preparation: parameters, protocols, and influence on virtual screening enrichments. *Journal of computer-aided molecular design*, *27*(3), 221–234. https://doi.org/10.1007/s10822-013-9644-8
69. Schrödinger Release 2023-4: Maestro, Schrödinger, LLC, New York, NY, 2023
70. Schrödinger Release 2023-4: Desmond Molecular Dynamics System, D. E. Shaw Research, New York, NY, 2023. Maestro-Desmond Interoperability Tools, Schrödinger, New York, NY, 2023
71. Seo, MH., Park, J., Kim, E. et al. Protein conformational dynamics dictate the binding affinity for a ligand. Nat Commun 5, 3724 (2014). https://doi.org/10.1038/ncomms4724
72. Singh, W., Karabencheva-Christova, T. G., Black, G. W., Ainsley, J., Dover, L., & Christov, C. Z. (2016). Conformational Dynamics, Ligand Binding and Effects of Mutations in NirE an S-Adenosyl-L-

Methionine Dependent Methyltransferase. Scientific reports, 6, 20107. https://doi.org/10.1038/srep20107

73. Sreedevi Chandrasekaran, Danail Bonchev,A NETWORK VIEW ON PARKINSON'S DISEASE, Computational and Structural Biotechnology Journal,Volume 7, Issue 8, 2013, e201304004,ISSN 2001-0370,https://doi.org/10.5936/csbj.201304004.
74. Tansey, M.G., Wallings, R.L., Houser, M.C. *et al.* Inflammation and immune dysfunction in Parkinson disease. *Nat Rev Immunol* **22**, 657–673 (2022). https://doi.org/10.1038/s41577-022-00684-6
75. Teilum, K., Olsen, J. G., & Kragelund, B. B. (2009). Functional aspects of protein flexibility. Cellular and molecular life sciences : CMLS, 66(14), 2231–2247. https://doi.org/10.1007/s00018-009-0014-6
76. Teng, X., Chen, S., Nie, Y., Xiao, P., Yu, X., Shao, Z., & Zheng, S. (2022). Ligand recognition and biased agonism of the D1 dopamine receptor. Nature communications, 13(1), 3186. https://doi.org/10.1038/s41467-022-30929-w
77. Wade, R. C., Gabdoulline, R. R., Lüdemann, S. K., & Lounnas, V. (1998). Electrostatic steering and ionic tethering in enzyme-ligand binding: insights from simulations. Proceedings of the National Academy of Sciences of the United States of America, 95(11), 5942–5949. https://doi.org/10.1073/pnas.95.11.5942
78. Werner, Milton & Olanow, C.. (2021). Parkinson's Disease Modification Through Abl Kinase Inhibition: An Opportunity. Movement Disorders. 37. 10.1002/mds.28858.
79. Whitworth, A. J., Lee, J. R., Ho, V. M., Flick, R., Chowdhury, R., & McQuibban, G. A. (2008). Rhomboid-7 and HtrA2/Omi act in a common pathway with the Parkinson's disease factors Pink1 and Parkin. Disease models & mechanisms, 1(2-3), 168–173. https://doi.org/10.1242/dmm.000109
80. Williams U, Bandmann O, Walker R. Parkinson's Disease in Sub-Saharan Africa: A Review of Epidemiology, Genetics and Access to Care. J Mov Disord. 2018;11(2):53-64.
81. Wishart DS. Improving early drug discovery through ADME modelling: anoverview. Drugs R 2007;8(6):349–62. https://doi.org/10.2165/00126839- 200708060-00003. PMID: 17963426.
82. Woon Bae Park, Sung Un Hong, Satendra Pal Singh, Myoungho Pyo, and Kee-Sun Sohn ACS Omega 2016 1 (3), 483-490 DOI: 10.1021/acsomega.6b00190
83. World Health Organization. (2019). Making the investment case for mental health: a WHO (No. WHO/UHC/CD-NCD/19.97). World Health Organization.
84. World Health Organization. (2022). Parkinson disease: a public health approach: technical brief.

Tables

Tables 2-5 are available in the Supplementary Files section

Figures

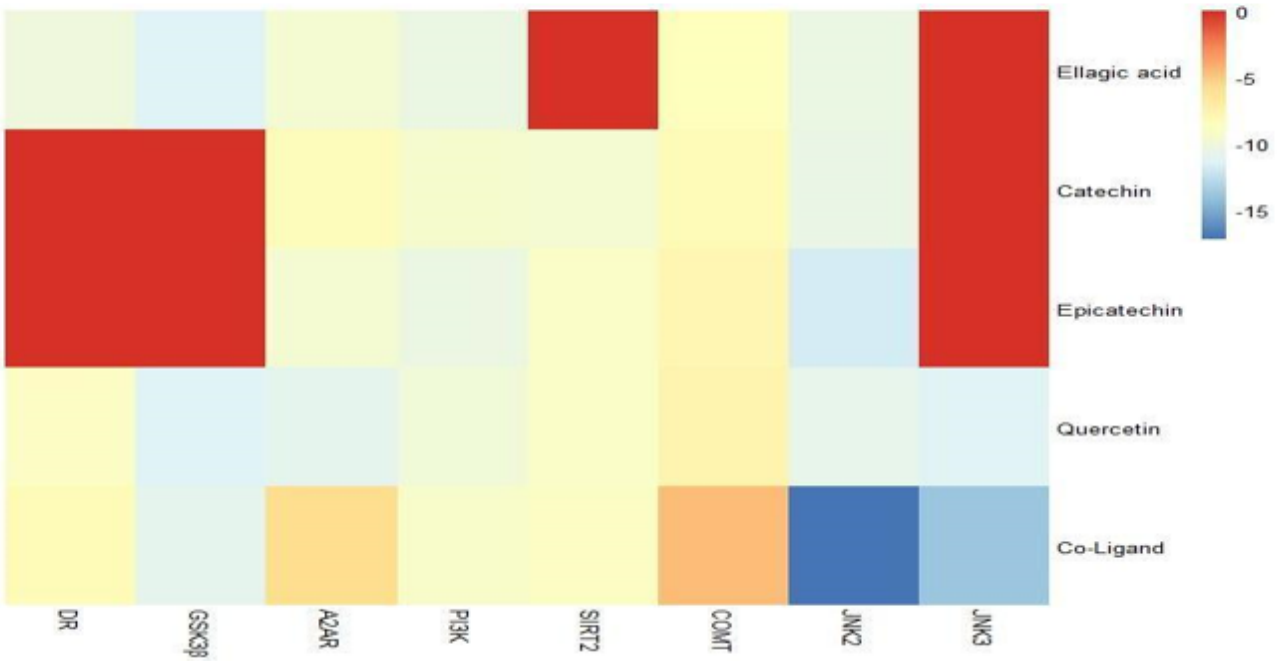

Figure 1

Heatmap showing the varying docking scores of the hit compounds against the lead targets.

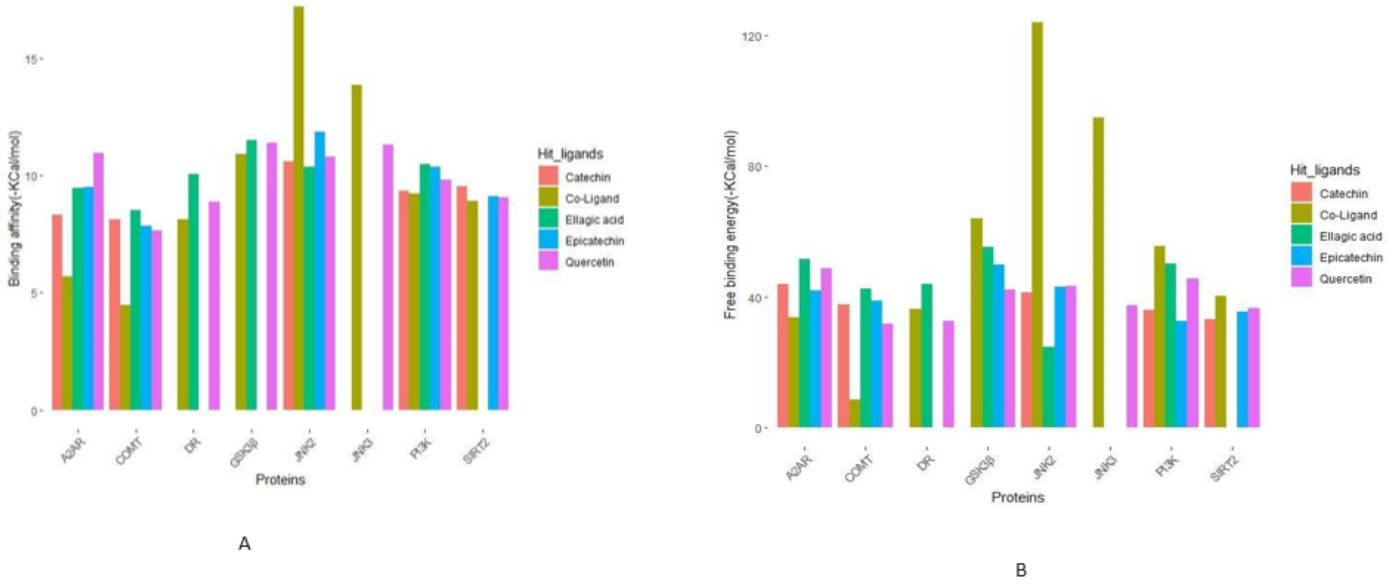

Figure 2

a: Bar-graph revealing binding scores(-kcal/mol) of the hit ligands against the lead targets.

b: Bar-graph showing the binding free energy(-kcal/mol) of the hit ligands against the lead targets.

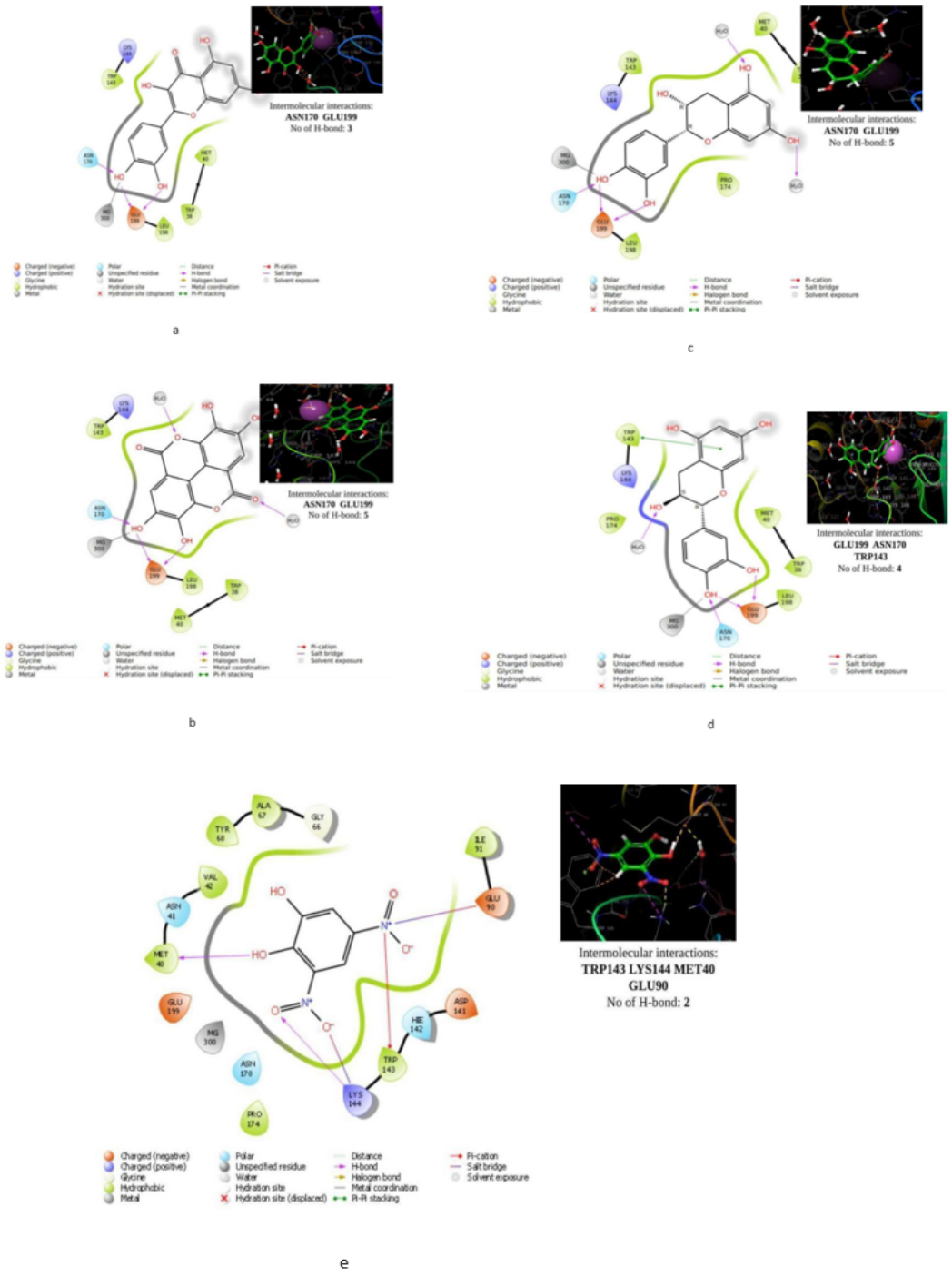

Figure 3

a: 2D and 3D plots of Quercetin interacting with the amino acid residues of Catechol-O-Methyltransferase

b: 2D and 3D plots of Ellagic acid interacting with the amino acid residues of Catechol-O-Methyltransferase

c: 2D and 3D plots of Epicatechin interacting with the amino acid residues of Catechol-O-Methyltransferase

d: 2D and 3D plots of Catechin interacting with the amino acid residues of Catechol-O-Methyltransferase

e: 2D and 3D plots of Co-ligand interacting with the amino acid residues of Catechol-O-Methyltransferase

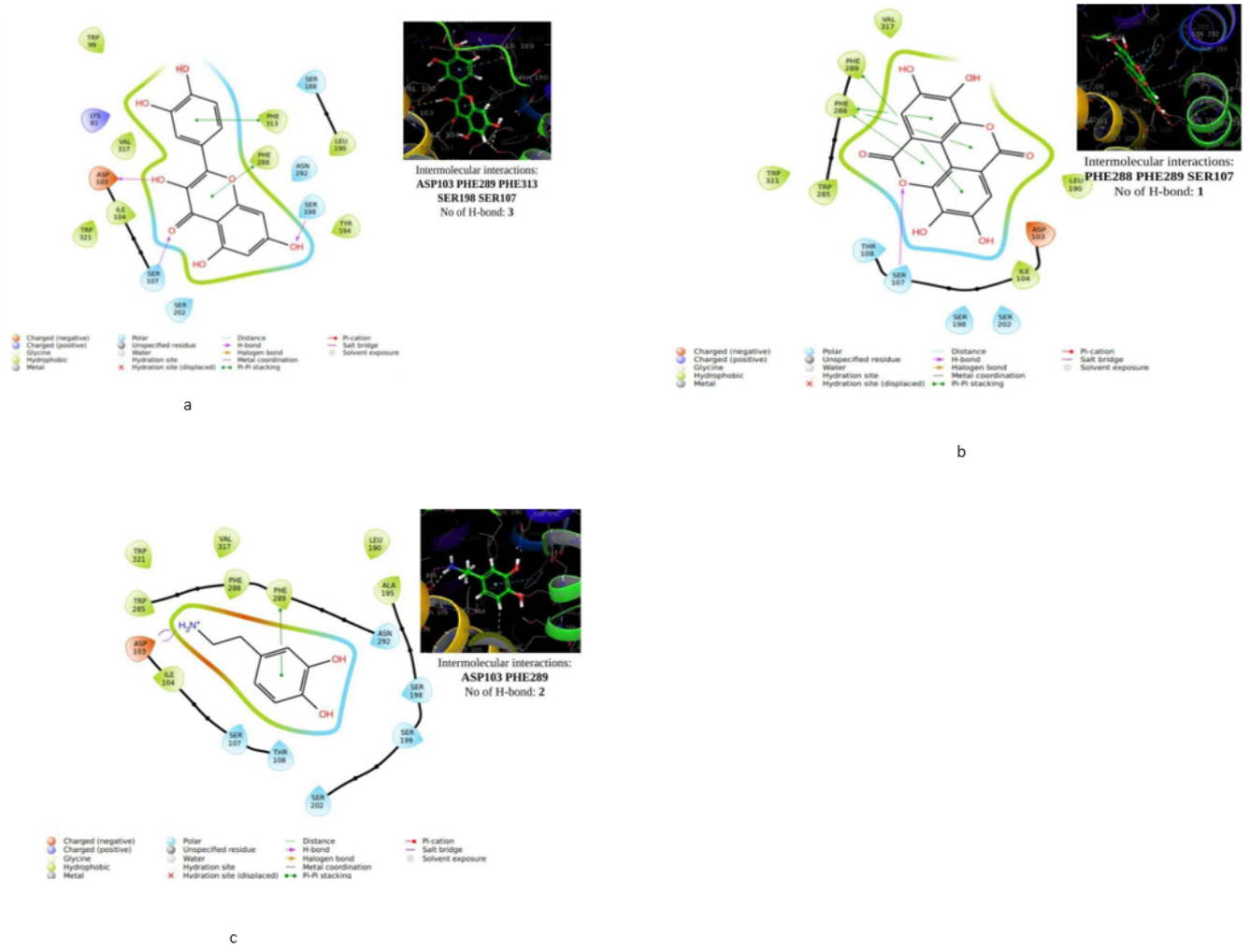

Figure 4

a: 2D and 3D plots of Quercetin interacting with the amino acid residues of Dopamine-D1 Receptor

b: 2D and 3D plots of Ellagic acid interacting with the amino acid residues of Dopamine-D1 Receptor

c: 2D and 3D plots of Co-ligand interacting with the amino acid residues of Dopamine-D1 Receptor

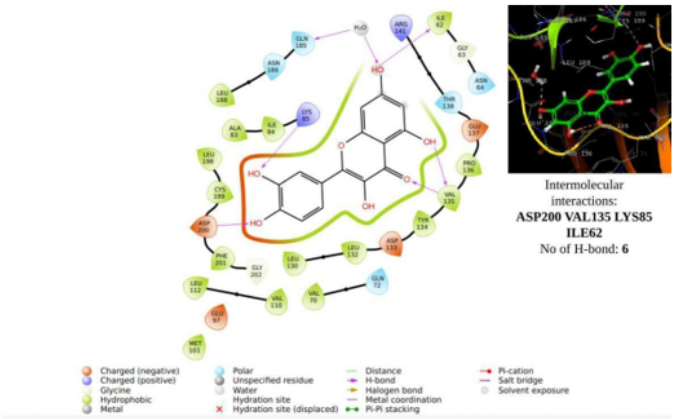

a

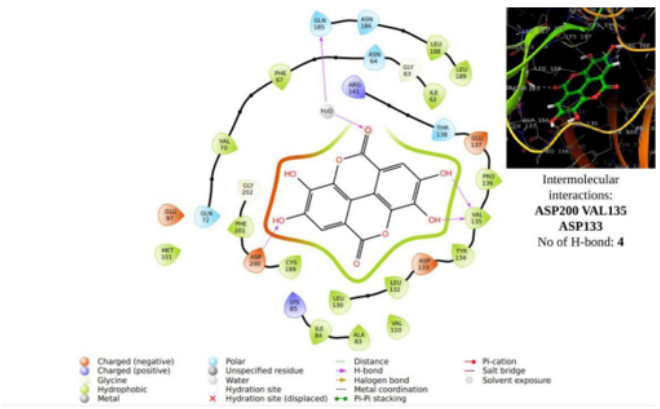

b

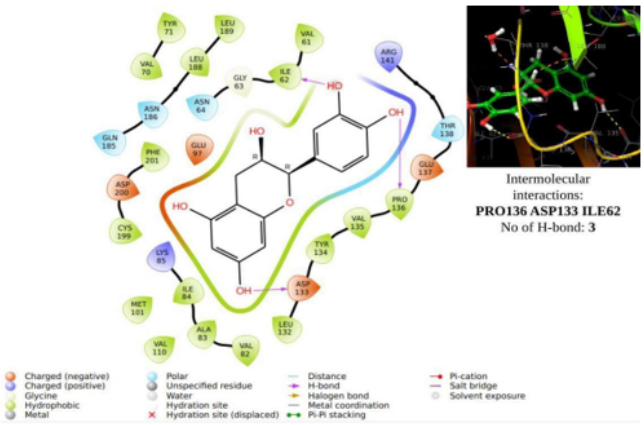

c

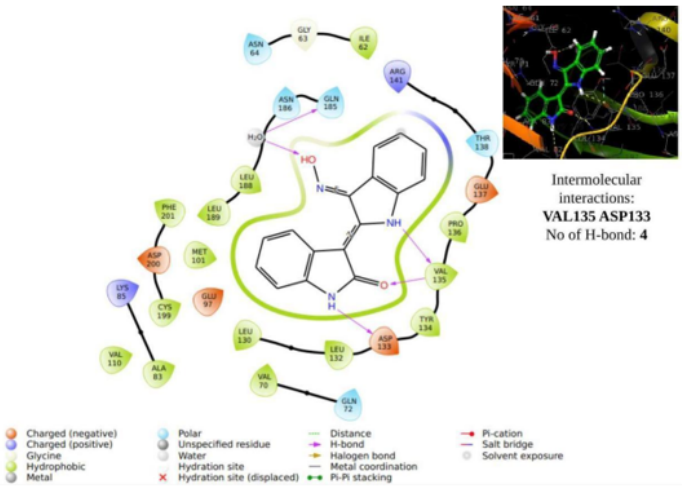

d

Figure 5

a: 2D and 3D plots of Quercetin interacting with the amino acid residues of GSK3β

b: 2D and 3D plots of Ellagic acid interacting with the amino acid residues of GSK3β

c: 2D and 3D plots of Epicatechin interacting with the amino acid residues of GSK3β

d: 2D and 3D plots of Co-ligand interacting with the amino acid residues of GSK3β

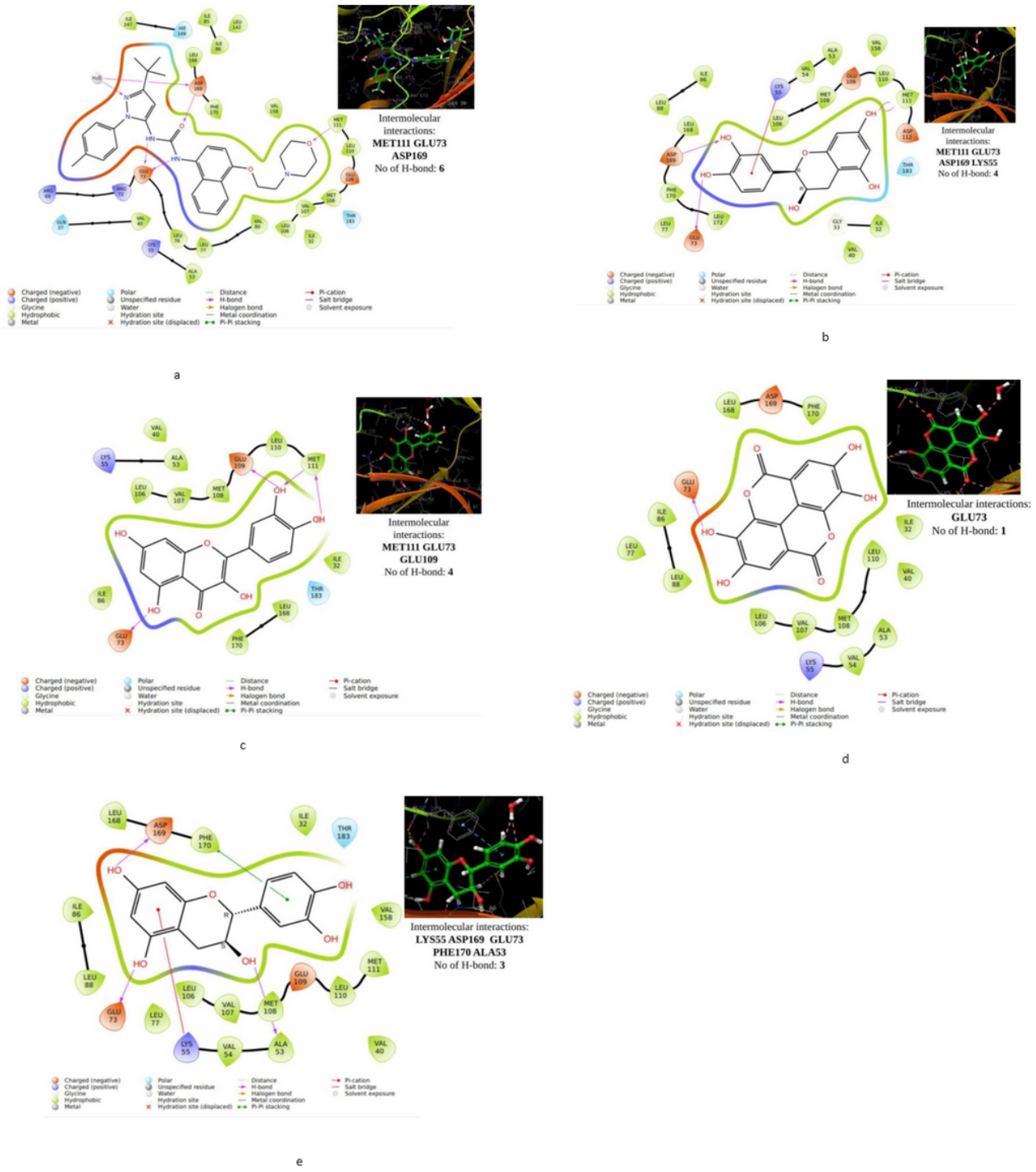

Figure 6

a: 2D and 3D plots of Co-ligand interacting with the amino acid residues of JNK2

b: 2D and 3D plots of Epicatechin interacting with the amino acid residues of JNK2

c: 2D and 3D plots of Quercetin interacting with the amino acid residues of JNK2

d: 2D and 3D plots of Ellagic acid interacting with the amino acid residues of JNK2

e: 2D and 3D plots of Catechin interacting with the amino acid residues of JNK2

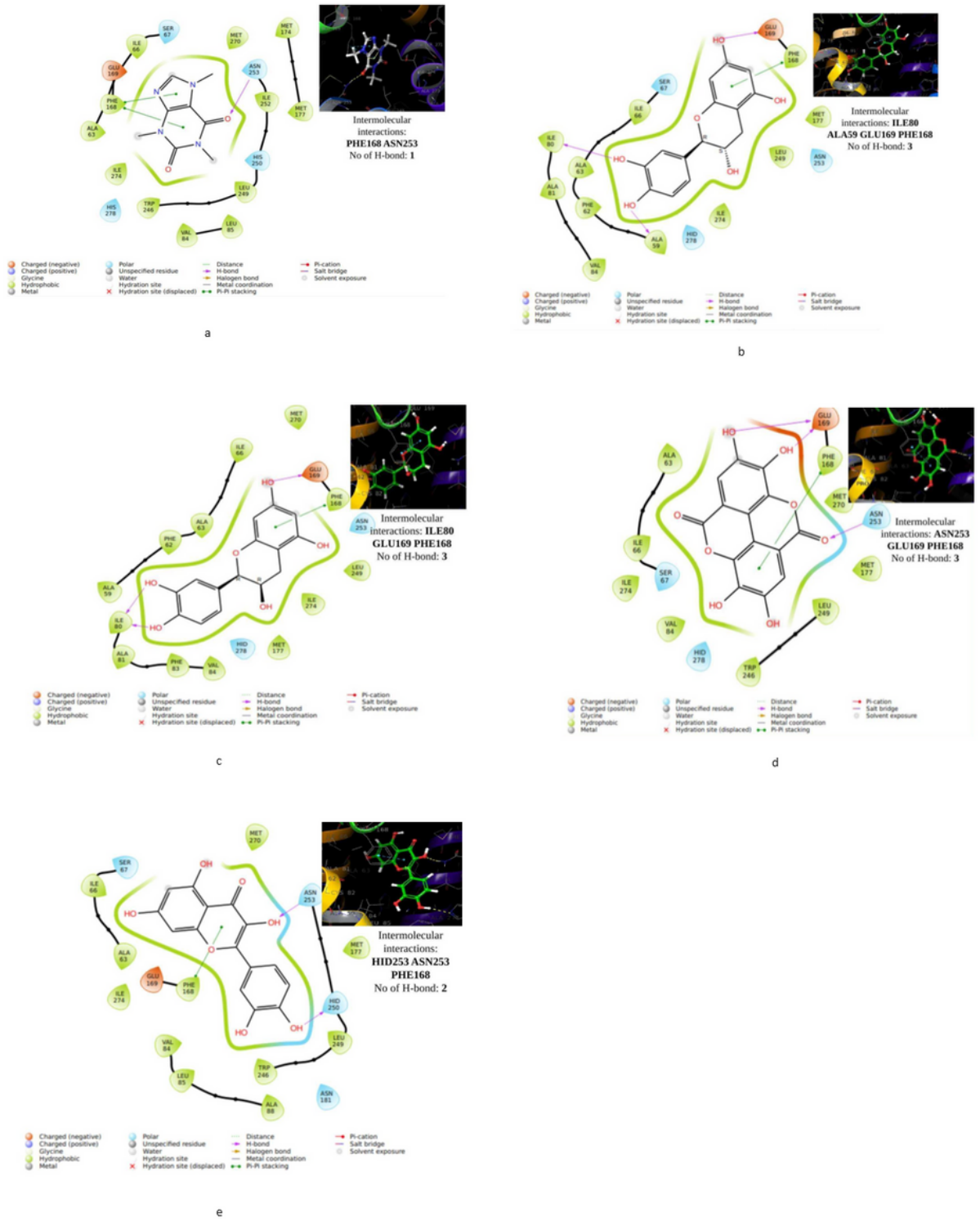

Figure 7

a: 2D and 3D plots of Co-ligand interacting with the amino acid residues of A2AR

b: 2D and 3D plots of Catechin interacting with the amino acid residues of A2AR

c: 2D and 3D plots of Epicatechin interacting with the amino acid residues of A2AR

d: 2D and 3D plots of Ellagic acid interacting with the amino acid residues of A2AR

e: 2D and 3D plots of Quercetin interacting with the amino acid residues of A2AR

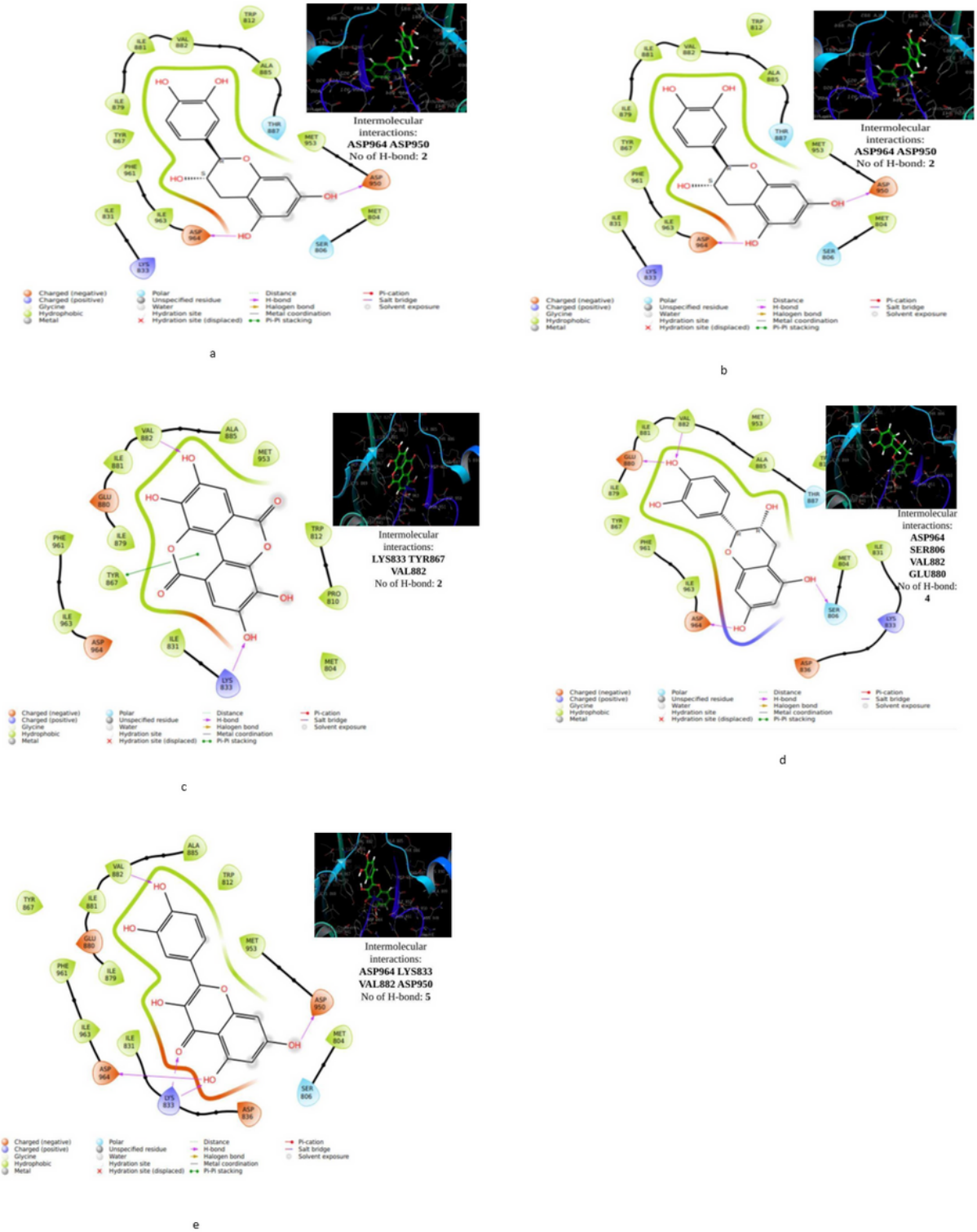

Figure 8

a: 2D and 3D plots of Co-ligand interacting with the amino acid residues of PI3K

b: 2D and 3D plots of Catechin interacting with the amino acid residues of PI3K

c: 2D and 3D plots of Ellagic acid interacting with the amino acid residues of PI3K

d: 2D and 3D plots of Epicatechin interacting with the amino acid residues of PI3K

e: 2D and 3D plots of Quercetin interacting with the amino acid residues of PI3K

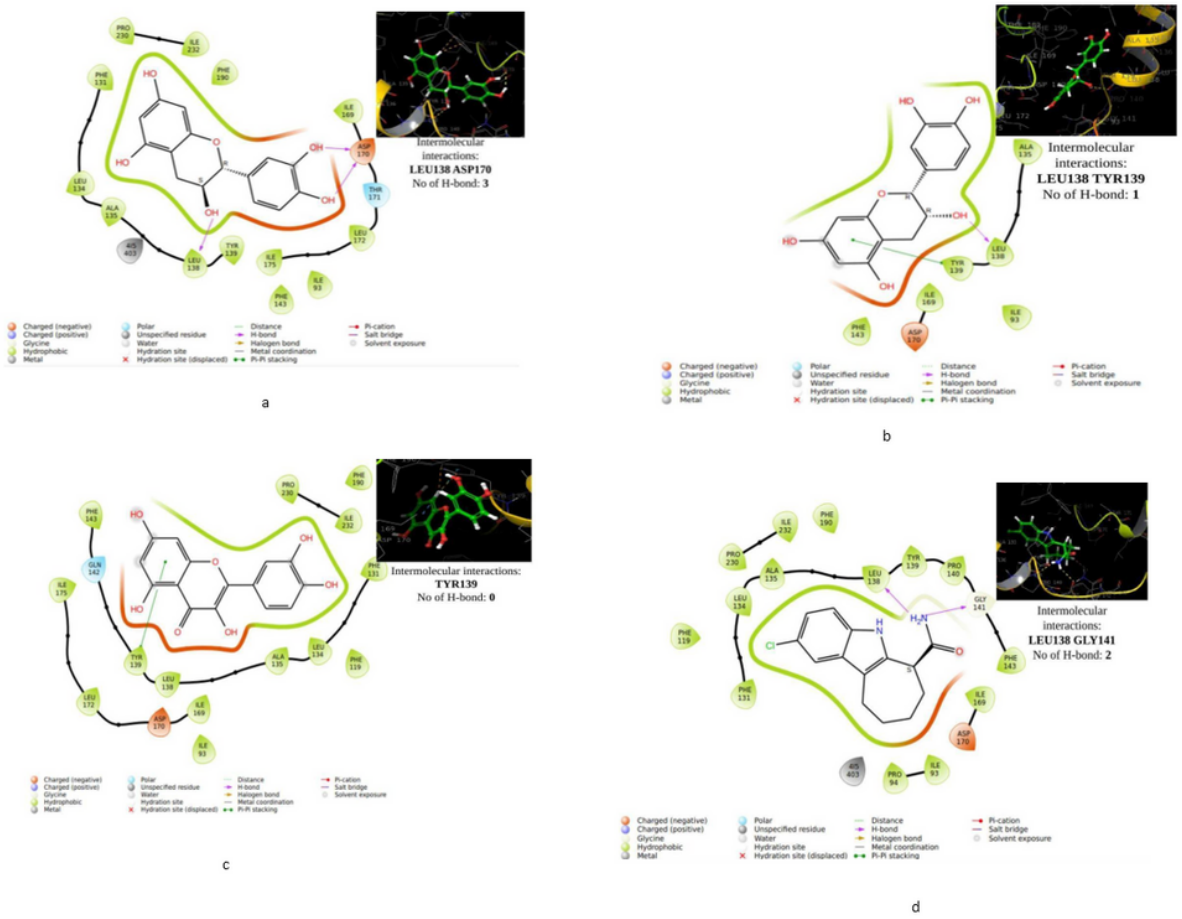

Figure 9

a: 2D and 3D plots of Catechin interacting with the amino acid residues of SIRT2

b: 2D and 3D plots of Epicatechin interacting with the amino acid residues of SIRT2

c: 2D and 3D plots of Quercetin interacting with the amino acid residues of SIRT2

d: 2D and 3D plots of Co-ligand interacting with the amino acid residues of SIRT2

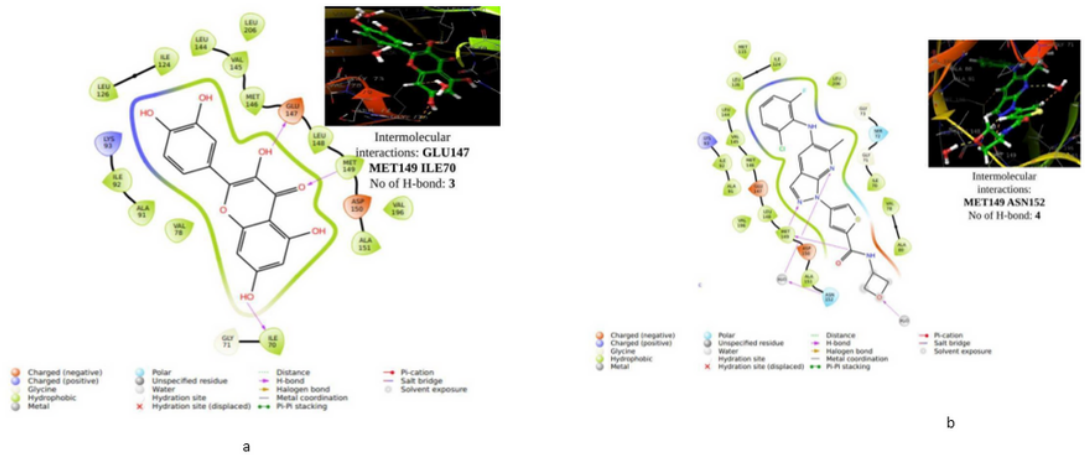

Figure 10

a: 2D and 3D plots of Quercetin interacting with the amino acid residues of JNK3

b: 2D and 3D plots of Co-ligand interacting with the amino acid residues of JNK3

Supplementary Files

This is a list of supplementary files associated with this preprint. Click to download.

- SupplementaryfileSpondias.docx
- GA.png
- Tables.docx